A Toy Model of Chemical Reaction Networks

Diplomarbeit

zur Erlangung des akademischen Grades

Magister rerum naturalium

an der
Fakultät für Naturwissenschaften und Mathematik
der Universität Wien

Vorgelegt von

Gil Benkö

im November 2002

meinen Eltern
nicht nur dafür, dass sie diese Arbeit ermöglicht haben

Dank an alle,

die zum Gelingen dieser Arbeit beigetragen haben:

Peter Stadler, Christoph Flamm, Ivo Hofacker, Peter Schuster, Othmar Steinhauser.
Ingrid Abfalter, Stephan Bernhart,Petra Gleiss, Kurt Grünberger, Ulli Mückstein, Stefan Müller, Johannes Soellner, Bärbel Stadler, Roman Stocsits, Andreas Svrcek-Seiler, Caroline Thurner, Andreas Wernitznig, Stefanie Widder, Christina Witwer, Michael Wolfinger, Judith Ivansits, Judith Jakubetz.
Alex, David, Dan, Irene, Marina, Martina, Monika, Patricija, Philipp, Roland, Stephanie, Sonne, Thomas, Waltraud.
Elisheva, Piter, Arad, Petra, Maria, Genia, Imre, Imre.
insbesondere an die Uni Wien für einen Reisezuschuß, Delores Grunwald (Computer Science Corp., Duluth MN) für den SMILES uniquetizer, Chemistry Development Project (`http://cdk.sourceforge.net`) für den SDG Algorithmus, Rob Tougher für die Socketklasse und Petra Gleiss für die Graphen-klasse.

Abstract

Chemical reactions networks (CRN) occur in our metabolism, in planetary atmospheres, they are used in combinatorial chemistry, and in the study of chemical decay processes. We want to study the properties these networks have in common by simulating them. Available simulations range from chemically accurate quantum mechanical simulations to artificial chemistries like the λ-calculus, with transparent dynamics. The one extreme is slow and difficult to analyze, while the other extreme does not include thermodynamics and other important features of chemistry.

Our model represents an intermediate level of abstraction. In analogy to the tree representation of the secondary structure of RNA, three-dimensional molecules are reduced to the topology of their graph representation. Using a parametrized Extended Hückel Theory, the graphs can then be submitted to a simple quantum mechanical wave function analysis. This yields for every graph an energy, its charge distribution, and molecular orbitals. Additionally, reaction mechanisms are abstracted by graph rewriting rules. The set of these rules thus specifies the chemistry of a CRN, i.e. its combinatorics. Directed by the energy and wave function shape of the reactants for every reaction, rewriting rules may be repeatedly applied. Thus a reaction network is generated from an initial set of molecules.

The aim of this model is to provide a consistent framework in which generic properties of a chemical reaction network can be explored. Two example networks have been built and studied. A repetitive Diels-Alder network was shown to be scale-free and small-world, while the formose reaction network displayed both properties less pronouncedly.

Zusammenfassung

Chemische Reaktionsnetzwerke (CRN) dominieren unseren Stoffwechsel, planetäre Atmosphären, die kombinatorische Chemie und chemische Verfallsprozesse. Wir interessieren uns für die Eigenschaften, die diesen Netzwerken gemeinsam sind, und möchten sie durch Simulationen erkunden. Erhältliche Simulationen reichen von der quantenmechanischen Berechnung bis hin zu der künstlichen Chemie, z.B. dem λ-calculus und seiner transparenten Dynamik-Darstellung. Während das erstere ein Extrembeispiel für schwierig zu analysierende, langsame Berechnungen ist, fehlen dem anderen Extrem thermodynamische und andere wichtige Eigenschaften der Chemie. Unser Modell stellt einen Mittelweg der Abstraktion dar. Die dreidimensionalen Moleküle werden, analog zur Baumdarstellung sekundärer RNA-Strukturen, auf die Topologie ihrer Graphendarstellung reduziert. Diese Graphen werden einer Energie- und Reaktivitätsberechnung im Rahmen einer parametrisierten Extended Hückel Theorie unterworfen. Es ist infolgedessen nur logisch, auch chemische Reaktionen als deren Graphen-Pendants, und zwar als *graph-rewriting*-Regeln darzustellen. Die Menge dieser Regeln definiert die Chemie der erzeugbaren CRNs, d.h. deren Kombinatorik. Die *graph-rewriting*-Regeln können nämlich wiederholt angewendet werden, wobei eine Selektion nach Energie und Elektronenverteilung der Reaktanden stattfindet. Somit kann das Toy Model ausgehend von einer Liste von Startmolekülen ein CRN generieren.

Das Ziel dieses Modells ist es, konsistent und robust genug für eine Erforschung der generischen Eigenschaften chemischer Reaktionsnetzwerke zu sein. Zwei Beispiele wurden erzeugt und analysiert: ein Netzwerk aus repetitiven Diels-Alder-Reaktionen und die Formose Reaktion. Vor allem das erstere, weniger das letztere, wiesen Merkmale von *scale-free*- und *small-world*-Netzwerken auf.

Contents

Chapter 1

Introduction

Networks of chemical reactions (CRNs) occur in many different areas (fig. 1.1). Looking at ourselves, we notice that our metabolism is governed by the interplay of pathways, i.e. chains of chemical reactions responsible for constructing and clearing the different parts of the organism. This interplay builds *metabolic networks* [35]. Looking back in time, we see that CRNs extend to hypercycles, reaction networks of self-reproducing molecules, which are considered to be the predecessors of life. Looking further back, the conditions making life possible are again CRNs, that have evolved since the formation of our planet. For example, the steady-state of the oxygen concentration in the atmosphere is now regulated by a set of reactions taking place in the sea, the air and in the earth's crust.

Man-made CRNs are as important as natural ones, especially from an economic point of view. Most importantly, a lot of effort has been put into the study of combustion [105], especially in the petroleum and the automobile industry. CRNs also have to be taken into account by chemical engineers for the construction of industrial-size chemical reactors. On the laboratory scale, the new fields of combinatorial chemistry and multi-component reactions use CRNs more complicated than a multi-step process for organic synthesis. At the interface of industry and nature, CRNs occur in chemical decay processes and are studied for their effects on the environment.

The diversity of CRNs spawns vast areas of research in the corresponding fields. Metabolic networks are studied in the life sciences, on the molecular and the pathway level (molecular and structural biology), and on the level of the network and its dynamics (systems biology). Their origin and evolution is the subject of astrobiology, and they are put to industrial use by biotechnology.

By analyzing metabolic networks it is possible to comprehensively understand the behavior of biological CRNs, i.e. how they maintain physiological

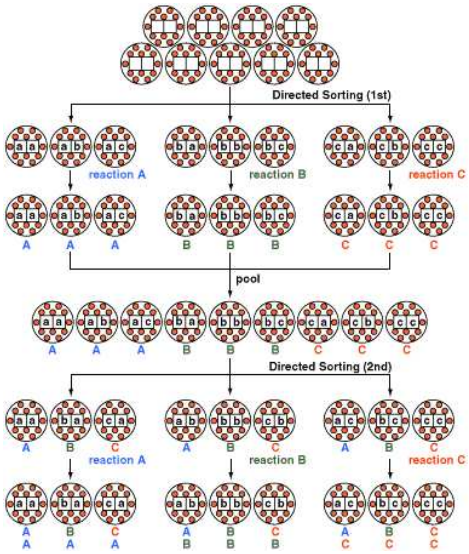

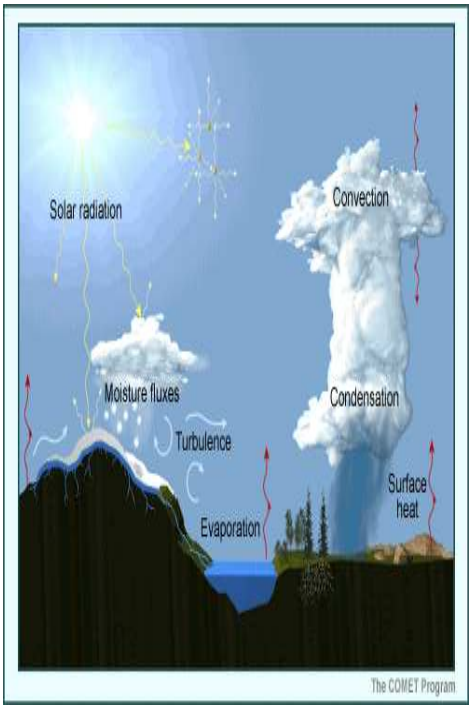

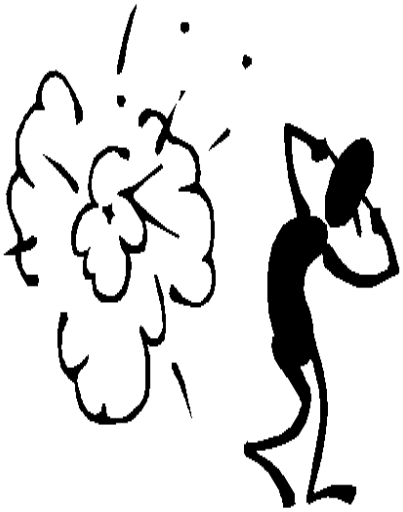

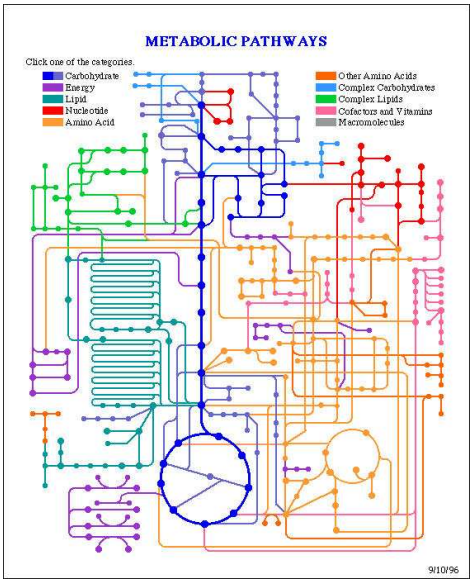

Figure 1.1: From top left: CRNs occur in combinatorial chemistry, atmospheric processes, combustion, and metabolic networks.

levels of metabolites (regulation) or may be influenced by external factors (control). *Control analysis* [58] and thermodynamic analysis of flows [79] provides a measure for the influence of a single reaction on the fluxes in the whole CRN. The related *flux analysis* [35, 21] defines for that purpose the flux coefficient, and, for the dependence on substrate or external concentrations, elasticities and response factors, respectively. Further analysis then yields steady states, and further structural analysis reveals constant elements (maximal conserved moieties), conservation relations and elementary modes of a CRN. Maximal conserved moieties are elements of species common to a group of species, remaining unchanged as the species transform into another. Conservation relations are linear combinations of species concentrations that are constant in time. Finally, elementary modes are parts of a CRN whose fluxes can be isolated independently. They are especially interesting for biotechnological applications aiming to increase these fluxes [106], and for understanding evolutionary optimization of metabolic networks [58].

The preceding paragraph showed how to analyze CRNs, i.e. how to extract information from a given CRN. But just as CRNs can be analyzed, they can also be synthesized. In this case CRNs are built from scratch or simulated *in silico*. The way a network develops may be observable by building it from minimal premises, and even afford predictions. On the other hand, a simulation is valuable as a substitute for potentially more complicated experimental studies. In ch. 2, a survey of CRN "synthesis" describes this research area.

Due to the diversity of CRNs, it is of immediate interest to determine which structural features are *generic properties* of large-scale reaction networks and which properties are the consequence of a particular chemistry. The graph-theoretic study of the structure of CRNs has been started by Balandin [9] and has been continued by the research on the enumeration and classification of CRNs [110].

The study of generic properties of CRNs is more recent and has identified many small-world networks among them [118, 1, 55]. This means that the graphs spanned by these networks have only short paths between any of their nodes. This observation would be made more meaningful by comparison with a generic CRN. It could be investigated if any random CRN and not only a specific network has small-world properties. Other interesting properties would be the scaling behavior, the network diameter, or the network center, for example.

The goal of this thesis is to model chemical reactions networks. The model should simulate how molecules of different constitutions, that determine their reactivity, are combined to a network of interconnected reactions. Eventually, we are interested in generic properties of a chemical reaction network by

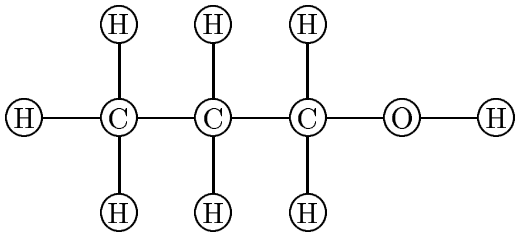

Figure 1.2: Alexander Crum Brown's master's thesis [14, 69] was the first scientific publication to use systematically the graph representation of molecules in today's form.

unbiased construction.

There are many models simulating different parts of CRNs at different accuracy levels (see sect. 2). The present Toy Model could be situated on a medium level of abstraction. QM/MM simulations, which use 3D information, are chemically more accurate, but may suffer from high time complexity. On the other hand, very abstract artificial chemistries are useful to study the evolution of networks but, like the λ-calculus (sect. 2.1), do not include thermodynamics or other important features of chemistry.

In chemistry, the changes of molecules upon interaction are not limited to quantitative properties of physical state, such as free energy or density, because molecular interactions do not only produce more of what is already there. Rather, novel molecules can be generated. This is the principal difficulty for any theoretical treatment of the situation. Chemical combinatorics makes it impossible to think of molecules as atomic names whose reactive relationships are tabulated. A computational approach to large scale reaction networks therefore requires an underlying model of an *artificial chemistry* to capture the unlimited potential of chemical combinatorics. The investigation of generic properties of chemistries requires the possibility to vary the chemistry itself; hence a self-consistent albeit simplified combinatorial model seems to be more useful than a knowledge-based implementation of the real chemistry which inevitably is subject to sampling biases.

We are going to use a graphical representation of molecules in connection with a simple quantum mechanical wave function analysis. The analysis determines the reactions and dynamics of CRN. This **Toy Model** of chemistry is computationally inexpensive and still retains the "look and feel" of the real (detailed quantum-mechanical) thing. In the following, the Toy Model is briefly described.

The representation of molecules as graphs has been used by chemists since the nineteenth century (fig. 1.2). In textbooks and scientific publica-

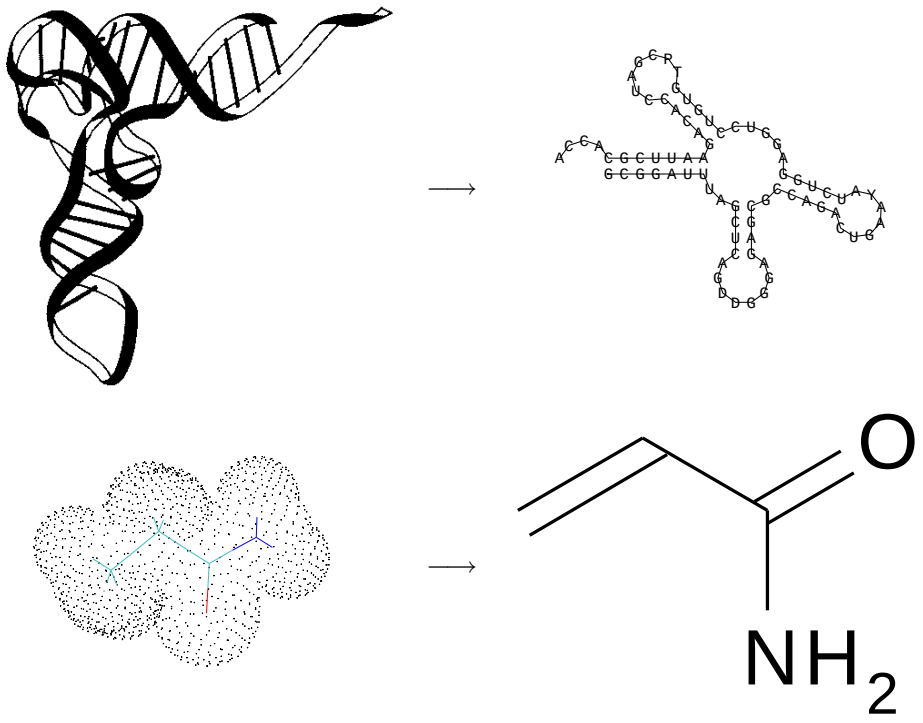

Figure 1.3: Analogy between the reduction of a RNA structure to its secondary structure (top, tRNA) and the reduction of a molecule to its graph representation (bottom, propenamide).

tions, the natural way for a chemist to describe a molecule is a graph. The nodes of graph are the atoms and the edges are the bonds. The graph reflects and was the first to explain the phenomenon of constitutional isomery [14]. Indeed, the description of molecular structures is one of the roots of graph theory [17, 108]. However, molecules can also be viewed as an agglomeration of atoms or nuclei in three-dimensional space. Most computational chemistry software packages implement molecules as a list of nuclei or atoms with three-dimensional coordinates. The position of the electrons, i.e. the electron distribution is then calculated as a charged cloud floating between the nuclei. Nevertheless, it can be argued that in the graph representation, the edges or bonds are already an educated guess on the electron distribution. Thus the loss of steric information in the graph representation might not be as radical.

The reduction of a three-dimensional molecule to the topology of its graph is somewhat analogous to the secondary structure model of RNA (fig. 1.3). The latter is also a reduction of the complete quaternary three-dimensional molecular structure to a tree representation. Three-dimensional coordinates

and symmetries are ignored. It nevertheless leads to excellent qualitative predictions of thermodynamic properties [61].

The graph representation of the molecule is now combined with a simple energy calculation. This suffices to fulfill the requirements of the laws of mass and energy conservation. It is then straightforward to represent reactions by graph rewritings (see ch. 2 and 4). The graph rewriting rules correponds to the reaction mechanism as understood by chemists. The Cannizarro reaction [16], for example, takes place between two aldehydes and produces an acid and an alcohol by disproportionation. The graph rewriting rule is analogous and adds a solvent proton node and a hydride node to one aldehyde graph to form an alcohol graph. The second aldehyde graph looses the former hydride node and gains a hydroxyl group (formed by two nodes), thus yielding the acid. The advantage of this reaction representation is that it represents the reaction itself also by graphs, and thus does not have the inherent limitations of e.g. string representations. It is also, of course, more flexible and simpler than a hard-coded implementation of reactions as complicated reactions might be very time-consuming to encode one per one.

Chapter 2

Artificial Chemistries

In this section we very briefly survey artificial chemistry models. Tab. 2.1 compares different CRN models based on their implementation of the three components molecules, reactions and networks [26]. The models can also be categorized according to abstraction level and intended application. Very abstract models simulate artificial chemistries in which string or logical elements interact, like in the λ-calculus. There networks are built in a bottom-up approach to be studied phenomenologically. On the other hand, models for practical applications tend to be top-down. They concentrate on describing interactions and try to predict, for example, the time or space evolution of concentrations. Some approaches are further described in the following.

2.1 The λ-calculus

The λ-calculus is a proof theory of constructive logic. This area of logic studies proofs using the interaction of logical elements called λ terms. Every λ term may be applied to another λ term to generate further λ terms, i.e. the deductions. Thus λ terms can be interpreted as objects as well as functions. The λ-calculus studies those functions and their applicative behavior, and indeed was founded to develop a general theory of functions, providing a foundation for logic and parts of mathematics [20]. In the related field of computer science, Turing [112] showed that the λ-calculus is strong enough to describe all mechanically computable functions. Ref. [109] reviews models based on the λ-calculus.

In analogy to λ terms, molecules in chemistry can be viewed both as undergoing and fueling a reaction, i.e. reactants and reagents. This analogy was exploited in the base model of [40]. We will describe now features of this model. It consists of a well-stirred flow reactor of interacting functions

Table 2.1: Comparison of different CRN models.

Model	Molecules have: Topology	Molecules have: 3D coordinates	Reactions are: Rewrite rules	Reactions are: QM/MM	Dynamics are: Exhaustive generation	Dynamics are: Explicit collision
Toy Model	•		•		•	
Atomoid [130]	•			•	•	
EROS [50]		•			•	
Patel [83]	•		•			•
GoForth [129]	•		•		•	
CCM [68]	•		•		•	
Faulon [33]	•					•
λ-calculus [40]	•		•			
Polymer AC [8]	•		•			•
String AC [27]	•		•		•	
Lancet [75]	•				•	
ARMS [107]	•		•		•	
Automata [66, 91, 128]	•		•			

$$\overbrace{(\overbrace{\lambda x.((x)\lambda y.y)x}^{A})\overbrace{\lambda u.(u)\lambda v.v}^{B}}^{\text{normalization/reaction completion}} \rightarrow$$

$$\overbrace{((\lambda u.(u)\lambda v.v)\lambda y.y)\,\lambda u.(u)\lambda v.v \rightarrow ((\lambda y.y)\lambda v.v)\,\lambda u.(u)\lambda v.v \rightarrow (\lambda v.v)\underbrace{\lambda u.(u)\lambda v.v}_{\text{“product”}}}^{\text{normalization/reaction completion}} \rightarrow$$

Figure 2.1: Example reaction triggered off by applying λ term A onto λ term B (after [42]). $(A)B$ denotes an application, and x, y, u, and v are “atomic names”. $\lambda x.A$ means that the λ term A is a function of x.

in the frame of the λ-calculus. λ terms are interpreted as molecules and interactions as chemical reactions. An interaction or deduction is carried out by a rewrite rule on the λ term. A non rewritable λ term is called a normal form and is equivalent to a stable molecule (fig. 2.1).

The λ-calculus can also be viewed as a formal theory of chemistry. Its advantage as an artificial chemistry is that it handles changes in the structure of an object, and that, moreover, the behavior of its objects depends on

their structure. Quantum mechanics also uses formal laws, but its consideration of molecules is too minute for an analysis of a CRN. The λ-calculus makes CRNs and the laws of their dynamics more transparent by using less detail. For example, CRNs or organizations of molecules do evolve in the λ-calculus. There is emergence of self-maintaining sets of functions, with a specific grammar defining their syntax, acting in accordance to invariant algebraic laws. They define a closure of interaction. In ref. [41], ecologies of different complexity levels are built.

Nevertheless, it is difficult to build a chemically sensible model of molecular decay in the λ-calculus. The model of [40] defines functions with finite lifetime, but in chemistry, the lifetime of molecules is understood to be determined by their reactivity and thus their structure. Although the Toy Model inherits the concept of rewriting from [40], it lets molecules decay based on their structure. Furthermore, the problem of molecular decay in the λ-calculus leads to violation of the law of mass conversation, and so does the lack of an equivalent of the chemical atom. A normalization, equivalent to reaction completion [42], shortens the λ term, and it is difficult to find a function that is preserved during a reaction, as an atom would be. Selective reactivity, multiple products, and rate constants, i.e. thermodynamics, also remain to be implemented into the calculus [42]. Terms in the lambda-calculus may always react and thus can build a chemical perpetuum mobile. The Toy Model addresses those issues and follows the simple bottom-up approach of the λ-calculus: simple data structures can be applied onto each other and may evolve into a complicated chemistry. In addition, the graph representation of molecules and a judicious choice of graph rewritings ensures mass conservation. Reactions can be encoded in graph rewritings in which the number and and mass of atoms and thus the total reactant mass does not change in the course of the reaction.

2.2 Atomoids, graphs, and matrices

The **Atomoid model** of [130] is inspired by the work of L. S. Penrose on self-reproducing mechanical models. It uses the graph representation for molecules, which are built from atoms connected by bonding hands. Bonding hands differ by energy level and energy structure. For a reaction to happen, it suffices that the connection of bond handles leads to an increase of energy of the bond handles. The reaction changes the atomic structure and the energy structure, which in turn changes the energy and may lead to the rupture of a distinct bond in the newly formed molecule. Bond handles may also interact via the exchange of photons. The photons are needed to avoid a freezing of

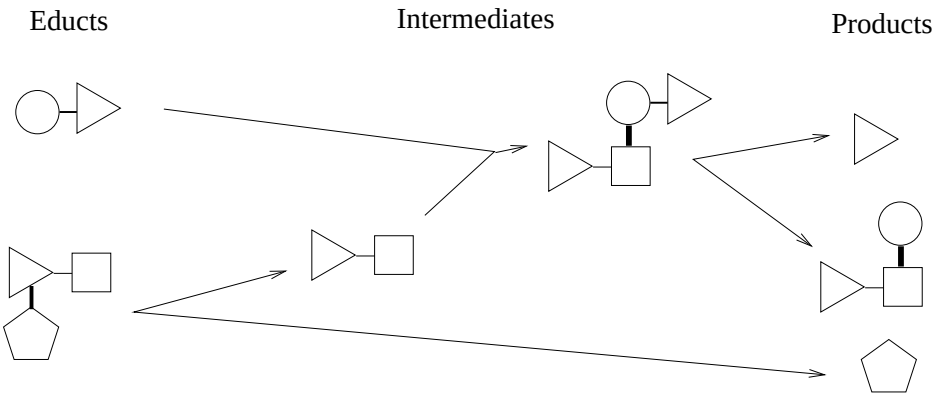

Figure 2.2: The Atomoid model. Molecules are built from "atoms" connected by bond handles differingin energy level and energy structure.

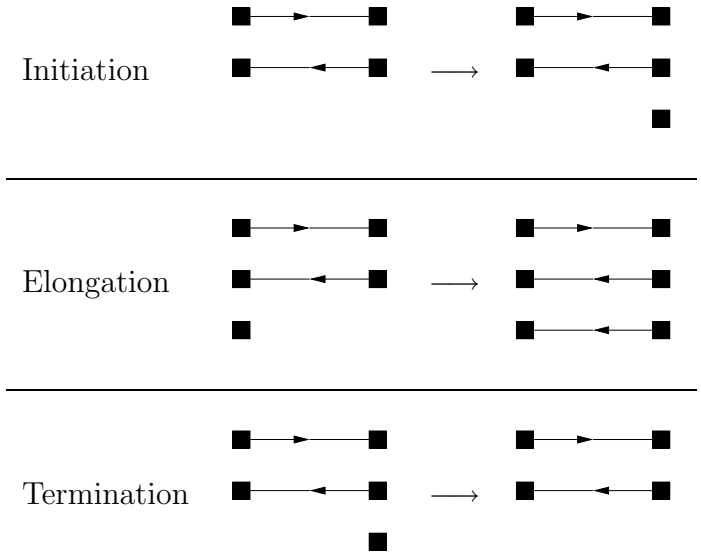

Figure 2.3: Simulation steps of RNA growth by the rewritable graph chemistry of [78].

the system from the start. These simple artificial atomic reaction rules lead to dissipative structures. The model enables one to follow on an atomic level how those dissipative structures lead to the emergence of self-reproductive hypercycles. Fig. 2.2 shows a simple example network.

The **rewritable graph chemistry** of [78], fig. 2.3, is designed to be complementary to the string-oriented analysis of nucleic acid polymers. The string editing is replaced by graph rewriting rules. They are encoded by subgraph graph replacements on labeled graphs called variable graphs, rep-

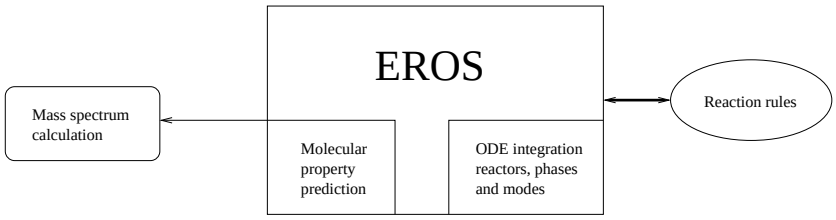

Figure 2.4: Modular organization of the organic chemistry simulation package EROS.

resenting chemical reactions. This model is used to simulate DNA and RNA transformations like enzymatic processing or combinatorial networks of catalyzed reactions. The model generates all possible derivation paths. It could be applied also to small organic molecules.

The **Iterated Graph Model** of [83] applies a limited subset of chemical reactions to a soup of molecules. Each chemical reaction, in this case food-browning reaction, is implemented as a separate function working on a molecular graph. The dynamics of the system are simulated by explicit collision. Pairs of molecules are chosen with a frequency proportional to their concentration in the soup and are submitted to a reaction function with a probability equivalent to the reaction rate. The reaction rates are fitted to match the evolution of the concentrations to experimental values.

EROS [50] is similar to the Toy Model by its straightforward implementation. Its basic architecture transparently reflects the three components molecules, reactions, and networks. The energy calculation for molecules involves are rule-based efficient generation of 3D coordinates, which makes it possible to accurately calculate many molecular properties. Reactions are hard-coded by two general reaction schemes. They are essentially pseudopericyclic σ and π electron shiftings whereby bonds are broken and formed. The CRN is generated exhaustively. The CRN generation can be combined with a "sifting-out of reactions", a model reduction based on reaction site properties, reaction enthalpy and reaction rates. EROS also implements phases, see fig. 2.4 for its module-oriented organization.

Approaches trying to avoid hard-coding reactions need to use a description of generic reactions [59]. The description used by the Toy Model is presented in sect. 4.1.

SMIRKS is a development of SMILES (sect. 3.3) capable of encoding generic reaction transforms as a line notation. However, rewrite rules are graphs and thus do not have the limitations of a line notation representation. Although all graph representations of generic reaction contain the same information [110, ch. 1], they differ by the stage or the part of the reaction

that is described. The imaginary transition structure [45] merges constant and changing parts into a single representation, while the skeleton of transformation [95] shows only the changing parts.

[83, 88] uses a hybrid approach with the Reaction Description Language. This language encodes the steps of reaction site identification, reaction matching, and reactant manipulation. The code is compiled and yields a hard-coded function for each reaction.

I. Ugi and coworkers [113, 114] have developed a a formal theory of chemical reactions called the **Dugundji-Ugi-model**. In this model, reactions are interconversions between isomers of 'ensembles of molecules' (EM). The concept of stoichiometric transformation in this model is used in the reaction simulation part of the Toy Model (see sect. 4.1). EM and reactions can be represented as matrices BE and R, such that the reaction R from BE_1 to BE_2 is equivalent to writing $BE_2 = BE_1 + R$. The off-diagonal entries of BE are bond orders between atoms, diagonal entries are number of valence electrons in lone pairs. Reaction generators (RG) may generate all R from a given BE_1 (RGB) or all BE from a given R (RGR). The program IGOR [39] is an RGR and generates new organic reactions and reaction networks between known educts and products. Koča et al. have developed an extension of the DU-Model, the synthon model [60, 73]. Here, lone electron pairs are represented by loops.

[33, 43] review methods to reduce the combinatorial explosion of possible reactions in formal models of CRNs. Reduction may be choosing a subset of reaction through an educated guess or in accordance to experimental observation. This subset may be a certain class of reaction, thus representing a special chemistry, or it may be formed by picking one representative reaction for each class of reactions. Finally, the subset used by [33] includes reactions according to their contribution to the reaction dynamics, by their concentration or by their rate constant. Thus the reaction mechanism reduction is achieved simultaneously with the CRN generation.

Chapter 3

Molecules

> The applicability of the EHM to large systems and to a variety of elements is one reason why it has been extensively applied to polymeric and solid-state structures.
>
> R. Hoffmann, Solids and Surfaces: A Chemist's View of Bonding in Extended Structures, VCH publishers, 1988.

3.1 Extended Hückel Theory

In quantum mechanics, electrons are described in terms of a wave function Ψ, which satisfies the time-dependent Schrödinger equation

$$\hat{H}\Psi = i\hbar\frac{\partial\Psi}{\partial t}, \tag{3.1}$$

where $\hat{H}$ is the Hamilton operator. If $\hat{H}$ is independent of time, Ψ satisfies the time-independent Schrödinger equation

$$\hat{H}\Psi = E\Psi, \tag{3.2}$$

where E is the energy of the system relative to the state in which the nuclei and electrons are infinitely separated and at rest.

A set of approximations leads to a computationally easily tractable problem:

The masses of the nuclei are much larger and their velocities much smaller than those of the electrons. In the **Born-Oppenheimer approximation**,

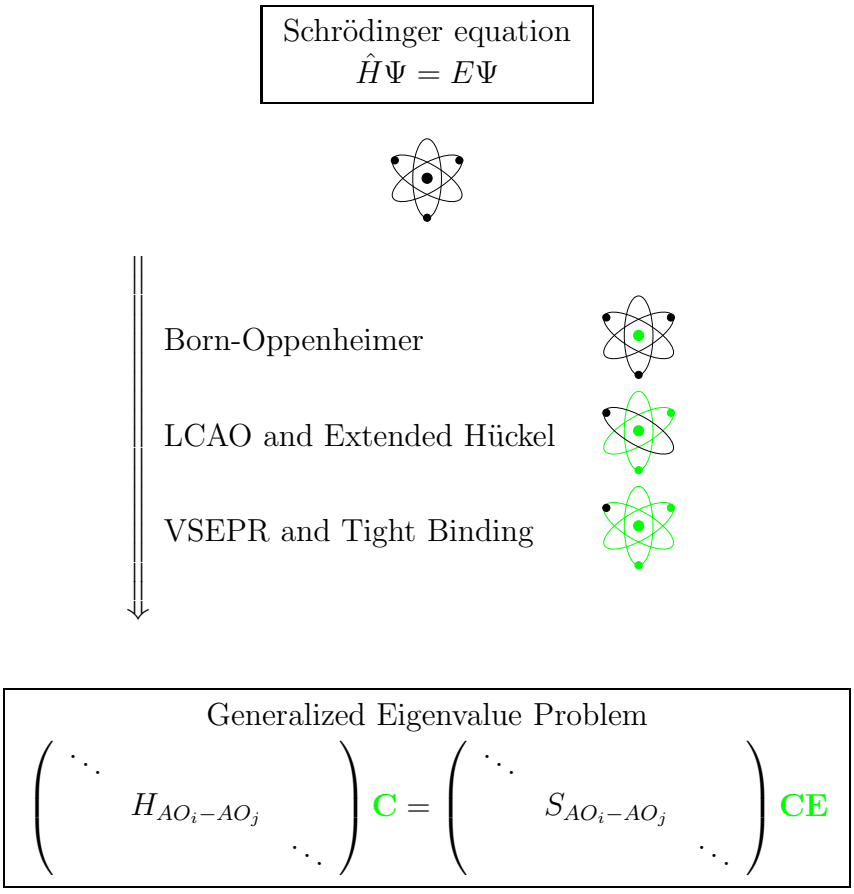

Figure 3.1: Schematic derivation of the used electronic calculation method. $H_{AO_i-AO_i}$, $S_{AO_i-AO_j}$ and K are given parameters (see equations 3.13).

the Schrödinger equation is separated into a part describing the electronic wave function Ψ_{el} for fixed nuclei,

$$\hat{H}_{el}\Psi_{el} = E_{el}\Psi_{el}, \tag{3.3}$$

and a part describing the nuclear wave function. The electronic Hamilton operator is:

$$\hat{H}_{el} = \sum_{i}^{e^-} \underbrace{\left(-\frac{1}{2}\hat{\nabla}_i^2 - \sum_{I}^{nuc}\frac{Z_I}{r_{iI}}\right)}_{\hat{h}_i} + \sum_{i}^{e^-}\sum_{j>i}^{e^-}\underbrace{\frac{1}{r_{ij}}}_{\hat{g}_{ij}} + \underbrace{\sum_{I}^{nuc}\sum_{J>I}^{nuc}\frac{Z_I Z_J}{r_{IJ}}}_{V_n}, \tag{3.4}$$

where $\hat{\nabla}$ is the nabla operator, Z_i is the nuclear charge of the atom i and r_{ij}

is the distance between the nuclei or electrons i and j. e^- and *nuc* indicate sums running over all electrons and nuclei, respectively. V_n, the electrostatic nuclear repulsion, does not depend on electron coordinates and is thus an additive constant to the final energy. For more clarity, it is omitted from the following equations.

Hartree proposed the **orbital approximation**, in which the wave function is built from Slater determinants,

$$\Psi_{SD} = \frac{1}{\sqrt{N!}} \begin{vmatrix} \phi_1(1) & \phi_2(1) & \cdots & \phi_N(1) \\ \phi_1(2) & \phi_2(2) & \cdots & \phi_N(2) \\ \vdots & \vdots & \ddots & \vdots \\ \phi_1(N) & \phi_2(N) & \cdots & \phi_N(N) \end{vmatrix} . \tag{3.5}$$

The ϕ are one-electron wave functions, called molecular orbitals (MO) or spin orbitals. The energy of a single Slater determinant will be used lateron for the variational principle. It may be written as

$$E_{el} = \int \Psi_{SD} \hat{H}_{el} \Psi_{SD} \mathrm{d}\,\tau \tag{3.6}$$

and decomposed into *one-electron* or *core* integrals $\int \phi_i(i) \hat{h}_i \phi_i(i)\,\mathrm{d}\tau$, *two-electron Coulomb* integrals $\int \phi_i(i)\phi_j(j)\hat{g}_{ij}\phi_i(i)\phi_j(j)\,\mathrm{d}\tau$, and *two-electron exchange* integrals $\int \phi_i(i)\phi_j(j)\hat{g}_{ij}\phi_j(i)\phi_i(j)\,\mathrm{d}\tau$.

Semi-empirical methods, **Extended Hückel Theory** [62, 65] for instance, now further approximate the wave function by building it from one single Slater determinant, thus neglecting electron correlation.

First, using the **basis set** or **LCAO approximation**, each ϕ is expanded as a linear combination of atomic orbitals χ (LCAO) :

$$\phi_i = \sum_j C_{ij} \chi_j \,. \tag{3.7}$$

The definition of the electron density ρ in LCAO will be needed in sect. 3.4 and will be shortly presented here. The electron density or the probability of finding an electron in a MO ϕ_i, occupied by n_i electrons, at the position defined by the position vector $\mathbf{r}$ is

$$\rho_i(\mathbf{r}) = n_i \phi_i^2(\mathbf{r}) \,. \tag{3.8}$$

As the MO s are normalized, we have:

$$\int \rho_i(\mathbf{r}) d\mathbf{r} \;=\; n_i \int \phi_i^2(\mathbf{r}) d\mathbf{r} = n_i \,.$$

Thus

$$\begin{aligned} \int \rho_i(\mathbf{r}) d\mathbf{r} \;&=\; n_i \sum_{j,k \in AO} C_{ji} C_{ki} \int \chi_j \chi_k d\mathbf{r} \\ &\Rightarrow \sum_{j,k \in AO} C_{ji} C_{ki} S_{jk} = 1 \,. \end{aligned} \tag{3.9}$$

Now, neglecting electron-electron repulsion $\hat{g}_{ij}$, the Hamilton operator is approximated as a sum of one-electron operators:

$$\hat{H} = \sum_i \hat{h}_i \,. \tag{3.10}$$

This gives the total energy as a sum over the one-electron energies of occupied molecular orbitals. Using the variational principle, which states that the best molecular orbitals are those that minimize the energy, we obtain a generalized eigenvalue problem:

$$\mathbf{HC} = \mathbf{SCE}, \tag{3.11}$$

where $\mathbf{C}$ is the matrix of the LCAO coefficients in eq. 3.7, $\mathbf{E}$ is the diagonal matrix of one-electron energies, and

$$\begin{aligned} H_{ij} \;&=\; \int \chi_i \hat{H} \chi_j \mathrm{d}\tau \\ S_{ij} \;&=\; \int \chi_i \chi_j \mathrm{d}\tau \,. \end{aligned} \tag{3.12}$$

Finally, the H_{ij} are parametrized:

$$\begin{aligned} H_{ii} \;&= -I_i \\ H_{ij} \;&= -\kappa \left(\frac{I_i + I_j}{2} \right) S_{ij} \,, \end{aligned} \tag{3.13}$$

in terms of the overlap integrals S_{ij}, the Wolfsberg-Helmholtz constant κ, and the *atomic valence state ionization potentials* I_i.

Theories related to Extended Hückel theory have been reviewed in [103]. Hückel-type calculations were first applied to saturated systems by [100].

K. Fukui used a LCAO approach with hybridized valence orbitals (LCVO) and calculated energies, charge distributions and dipole moments. He used perturbation theory to develop from there the Frontier Molecular Orbital Theory (see sect. 3.6) and to calculate reactivities. Further refinements of EHT were made to account for electron-electron interaction. An iterative EHT (IEHC) was developed in order to obtain more accurate atomic charges. Electron-electron correlation is usually completely neglected but has been approximated by Atom Superposition and Electron Delocalization Molecular Orbital theory (ASED-MO) [4, 5], thus affording better prediction of geometries.

3.2 Further approximations

The basis set used for the LCAO is the $1s$ orbital for hydrogen and hybrid AOs for carbon, nitrogen and oxygen. Hybrid AOs are linear combinations of Slater-type orbitals, coefficients depending on the hybridization of the atom.

Tab. 3.1 shows the definition of Slater-type and hybridized orbitals used. Sulfur and phosphor would also require d-orbitals and their hybrids dsp^3 and d^2sp^3.

Hybrid orbitals are used because we can assume for simplicity that they are always oriented along bonds, such that for given atom types and hybridizations, there is always the same overlap. Thus, the corresponding overlap integral, instead of being calculated repeatedly, can be replaced by a constant parameter, in analogy to the Tight Binding approximation for solids [104]. This would not be the case for normal Slater-type orbitals.

A molecule is therefore completely determined by a vertex labeled graph g, which was introduced by O. Polanski [87]. A graph $g = (V, E)$ is a set of vertices V and a set of edges E. Vertices are elements v_i. Edges are pairs of vertices $(u, v) \in V \times V$ defining connected vertices. The vertices of g are the atom orbitals (labeled by atom type and hybridization); edges denote overlaps of orbital on adjacent atoms. This *orbital graph* g is obtained in an unambiguous way from the chemical structure formula by means of the rules described in the following. It follows that, in the framework of the Toy Model, the structure formula already encapsulates the complete information about the molecule.

The rules for constructing the orbital graph are:

- Overlaps are only non-zero (orbital graph edges exist only) between orbitals on connected atoms.
- Only the overlaps shown in figs. 3.4, (a) and (b) (direct σ, semi-direct),

Table 3.1: Definition of Slater-type (STO), sp^3-, sp^2- and sp-hybridized atomic orbitals. STOs are electron distributions, given here in spherical coordinates (r, θ, ϕ). $Y_{l,m}$ are the usual spherical harmonic functions and n, l, m define the orbital type. N is a normalization constant and ζ is a parameter, both varying with n, l, m and Z, the atomic number.

$$\chi_{\zeta,n,l,m}(r,\theta,\phi) = NY_{l,m}(\theta,\phi)r^{n-1}e^{-\zeta r} \qquad \text{(general form)}$$

STOs

$$\begin{aligned} 1s &= Ne^{-\zeta r} \\ 2s &= N(1-\zeta r)e^{-\zeta r} \\ 2p_x &= N\zeta r e^{-\zeta r}\cos\theta \\ 2p_{y,z} &= N\zeta r e^{-\zeta r}\sin\theta e^{\pm i\phi} \end{aligned}$$

sp^3 orbitals

$$\begin{aligned} \chi_1 &= \frac{1}{2}(2s + 2p_x + 2p_y + 2p_z) \\ \chi_2 &= \frac{1}{2}(2s + 2p_x - 2p_y - 2p_z) \\ \chi_3 &= \frac{1}{2}(2s - 2p_x - 2p_y + 2p_z) \\ \chi_4 &= \frac{1}{2}(2s - 2p_x + 2p_y - 2p_z) \end{aligned}$$

sp^2 orbitals

$$\begin{aligned} \chi_1 &= \sqrt{\frac{1}{3}}2s + \sqrt{\frac{2}{3}}2p_x \\ \chi_2 &= \sqrt{\frac{1}{3}}2s - \sqrt{\frac{1}{6}}2p_x + \sqrt{\frac{1}{2}}2p_y \\ \chi_3 &= \sqrt{\frac{1}{3}}2s - \sqrt{\frac{1}{6}}2p_x - \sqrt{\frac{1}{2}}2p_y \\ \chi_4 &= 2p_z \end{aligned}$$

sp orbitals

$$\begin{aligned} \chi_1 &= \frac{1}{\sqrt{2}}(2s + 2p_x) \\ \chi_2 &= \frac{1}{\sqrt{2}}(2s - 2p_x) \\ \chi_3 &= 2p_y \\ \chi_4 &= 2p_z \end{aligned}$$

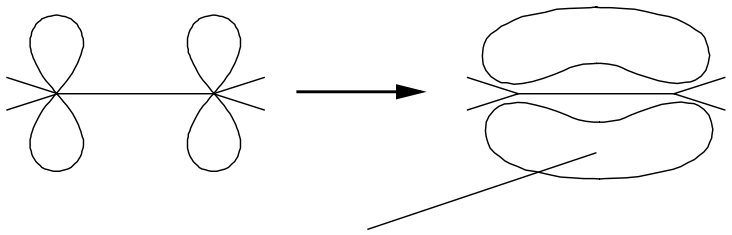

Figure 3.2: π-overlap between p orbitals.

3.2, and 3.3 (π, hyperconjugation and fictitious) are implemented. The other possible overlaps between hybridized orbitals, see fig. 3.4, (c) and (d) (indirect), are set to zero as they are in average as low as 0.1 .

- In the style of [89] and [86, ch. 6.4], the term hyperconjugation is used for overlaps between a p orbital and a neighboring, but "indirect" oriented sp^3 orbital. Only one of the three sp^3 is randomly chosen for an overlap proportional to the π overlap of the corresponding atoms. The other two "indirect" oriented overlaps are set to zero. In order to avoid choosing randomly an orbital, but to keep the σ-MOs and the π-system coupled, a second factor is defined for the overlap between the p orbital and the "direct" oriented sp^3 orbital. This factor may be used instead of the hyperconjugation factor. The overlap is dubbed "fictitious".

- The set of overlaps is determined by the hybridization of the two atoms involved in the bond. Tab. 3.2 shows all the possible combinations of hybridizations and ensuing overlaps. The set of overlaps only depends on the type and orientation of the orbitals.

Thus the energy calculation in the Toy Model is parametrized in terms

Table 3.2: Sets of overlaps depending of hybridization on bonding atoms.

Hybridization of		number of overlaps (see figs. 3.2, 3.3 and 3.4)				
atom 1	atom 2	σ	semi.	π	hyper.	fictitious
sp^3	sp^3	1	6	0	0	0
	sp^2	1	5	0	1	1
	sp	1	4	0	1	1
sp^2	sp^2	1	4	1	0	0
	sp	1	3	1	0	0
sp	sp	1	2	2	0	0

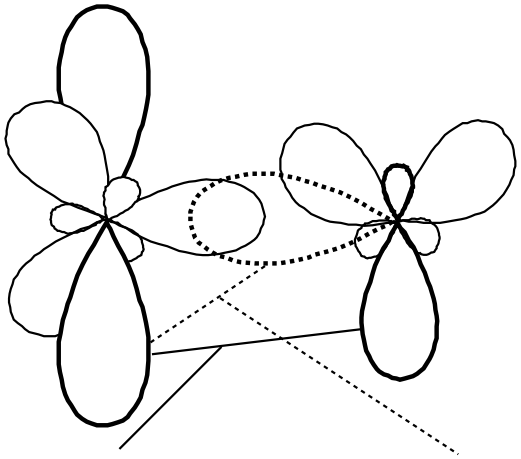

Figure 3.3: Hyperconjugation and artificial overlap between p and sp^3 orbitals.

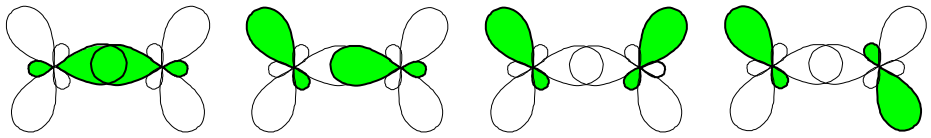

Figure 3.4: Overlap along a bond (a), "semi-direct" overlap, where only one of the orbitals is directed along the bond (b), and the two possibilities of "indirect" overlaps of two sp^2 orbitals at adjacent atoms (c,d). In the graph-theoretical model (c) and (d) are equivalent because the orientation in the plane is not a property of the molecular graph. In the case of a symmetric molecule, randomly assigning (c) and (d) could break the symmetry of the molecule, and moreover difficult to reproduce. In the current implementation "indirect" overlaps are neglected.

of ionization energies I_j and overlap integrals S_{ij} of the usual Slater-type hybrid orbitals. The numerical values are listed in appendix A. The S_{ij} for direct overlaps are given explicitly in the appendix, the other overlaps are parametrized using simple scaling factors applied on the direct overlaps, see tab. 3.2. The factor used to calculate the semi-direct overlap from the direct overlaps depends on whether one of the bonded atoms is a hydrogen.

Calculations (see appendix A) show that the approximation by this scaling factor is inaccurate. However, it is kept for simplicity, but might be later replaced by an independent set of parameters.

The overlaps over bonds which lie in three- and four-membered rings

are also scaled by factors. This reflects the weakness of "banana-bonds" in constrained rings. The factor 3-ring applies to all bonds in a three-membered ring. The factor 4-ring applies only to other bonds in four-membered rings, in order to reflect that bridging bonds, i.e. bonds contained in two rings, are as strained as bonds in three-membered rings (more precise data is available from [11]).

The hybridization of a particular atom is determined using valence-shell electron pair repulsion (VSEPR) theory [53]. VSEPR is a simple method to predict the geometry of compounds. The only thing needed is the connectivity of the compounds, which is given by definition by the graph representation of the molecule. The VSEPR theory assumes that the valence-shell electron pairs of any atom in the molecule are arranged in a fashion that minimizes electrostatic repulsion. Electron pairs are represented by the bonds, i.e. edges of the molecular graph, and by lone electron pairs, whose number depends only on what element the atom is. Every bond, be it simple, double or triple, counts as one electron pair. The geometry of atoms depends in the end on the number of electron pairs, in bonds and in lone pairs. A total of 2 leads to linear geometry and sp hybridization, 3 to trigonal geometry and sp^2 hybridization, and 4 to tetrahedral geometry and sp^3 hybridization. The atom on which VSEPR is applied is called the central atom. Tab. 3.4 summarizes the results and gives examples for neutral atoms and a charged central atom.

To account for resonance structures, a few more rules are added. Resonance structures occur when more than one Lewis structure can be drawn for a molecule. The most common situations are adjacent π bonds, and a lone pair adjacent to a π bond [86, sect. 6.3]. The former has been taken care of by always establishing π interactions between adjacent sp^2 atoms (see tab. 3.2). The latter corresponds to the situation where, when drawing alternative Lewis structures, lone pairs and π bonds are converted into each other. In fact, the electrons are *delocalized*.

Thus the hybridization of an atom with lone pairs depends on its neighbors, namely those who are not sp^3 hybridized. The current implementation

Table 3.3: Scaling factors for calculating remaining overlaps from the overlaps in Tab. A.2

indirect		hyper-		banana	
all	H	conjugation	symmetric	3-ring	4-ring
0.1	0.0	0.8	0.0	0.7	0.8

Table 3.4: Geometry of C, N and O according to VSEPR theory.

Atom	Number of e^- in bonds	lone pairs	total	Hybridization
C	4	0	4	sp^3
	3	0	3	sp^2
	2	0	2	sp
N	3	1	4	sp^3
	2	1	3	sp^2
	1	1	2	sp
O	2	2	4	sp^3
	1	2	3	sp^2
O^-	1	3	4	sp^3

Table 3.5: Resonance.

hybridization of connected atom	# of lone pairs on central atom	change in hybridization of central atom
sp^2	1	$sp^3 \rightarrow sp^2$
	2	$sp^3 \rightarrow sp^2$
sp	1	$sp^3 \rightarrow sp^2$ $sp^2 \rightarrow sp$
	2	$sp^3 \rightarrow sp$ $sp^2 \rightarrow sp$

starts from the latter atoms (central atom) and then looks for atoms with lone pairs which are connected over single bonds. The changes in hybridization resulting from resonance implemented in the Toy Model are shown in tab. 3.5.

The orbital graph resulting for propenamide is shown in fig. 3.5.

By the preceding method, the orbital graph and thus **H** and **S** are completely determined by the original chemical graph. It contains only information on atom types and connectivity, but this suffices to derive hybridizations and overlaps according to VSEPR. Per definition, any property may now be calculated for the molecule from its wave function (see sect. 3.4).

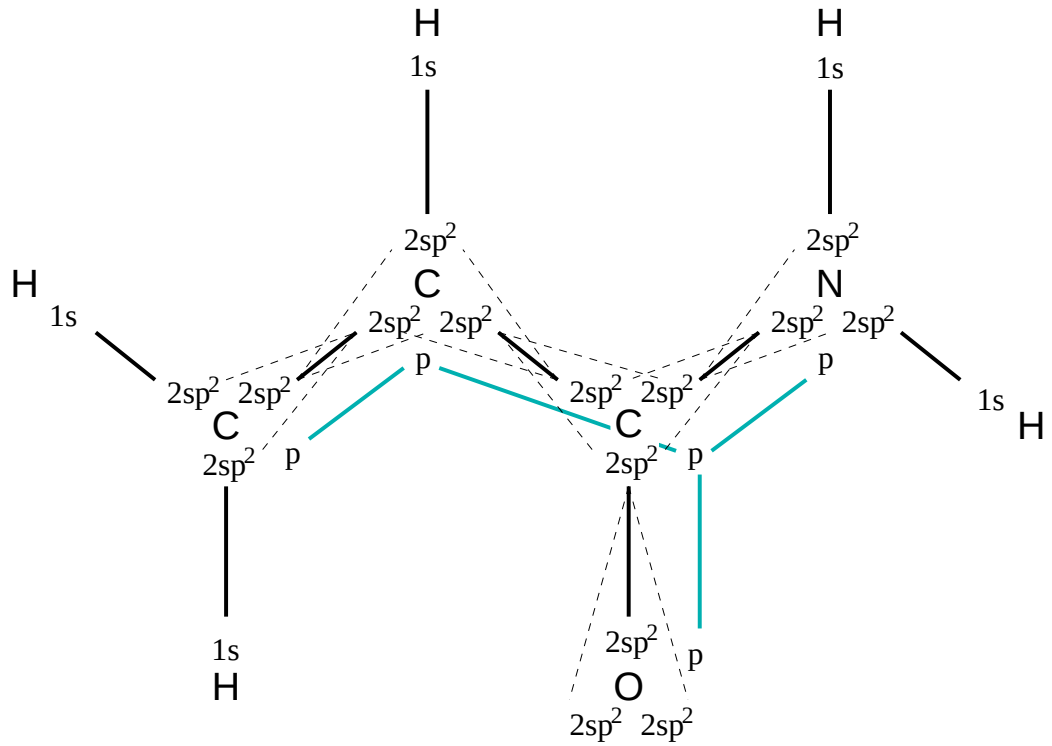

Figure 3.5: Orbital graph of propenamide $H_2C = CH - C(= O) - NH_2$. Direct, semi-direct σ-overlaps, and π-overlaps are represented by solid black, dashed, and solid gray lines.

3.3 Chemical structure representation

As the Toy Model only needs to store a graph to represent a molecule completely, an appropriate structure representation format has to be selected.

A particularly convenient encoding is the *Graph Meta Language* (GML) [90]. It is a simple and flexible file format for graphs, designed to represent arbitrary data types as ASCII files. The BNF notation for GML is:

```
GML         ::= List
List        ::= (whitespace* Key whitespace+ Value)*
Value       ::= Integer | Real | String | [ List ]
Key         ::= [ 'a'-'z'  'A'-'Z' ] [ 'a'-'z'  'A'-'Z'  '0'-'9' ]*
Integer     ::= sign digit+
Real        ::= sign digit* . digit* mantissa
String      ::= '"' instring '"'
sign        ::= empty | + | -
```

```
digit      ::= ['0'-'9']
Mantissa   ::= empty | 'E' sign digit
instring   ::= ASCII - {\&,"} | \& character+ ;
whitespace ::= space | tabulator | newline
```

Here, graphs are encoded by blocks starting with the keyword `graph`. Inside this block, nodes and edges are defined by key-value list using the keywords `node` and `edge`. The following example shows how their attributes are defined:

```
# Isobutane
graph [
  node [ id 1 label "C" ]
  node [ id 2 label "C" ]
  node [ id 3 label "C" ]
  node [ id 4 label "C" ]

  edge [ source 1 target 2 label "-" ]
  edge [ source 1 target 3 label "-" ]
  edge [ source 1 target 4 label "-" ]
]
```

Labels of atoms and bonds define their type, i.e. C, N, or O for atoms, and − (single), = (double), or # (triple) for bonds.

The GML format is precise and non-redundant, but long and tiresome to read. Thus, a different format is need for quickly displaying lists of molecules.

SMILES (Simplified Molecular Input Line Entry Specification)[1] is a line notation, i.e. a string representation for molecules. SMILES are compact and their grammar is easy to learn. Their similarity to structural formulae makes their grammar intuitive for chemists.

Moreover, in order to eliminate duplicates from a list of molecules or to subtract one list of molecules from another, as in sect. 5.1, a comparison of the structural formulae must be performed. This amounts to a test of graph isomorphism, for which neither an efficient algorithm nor proof of NP-completeness is known in general [72]. The chemically relevant problem of testing graph isomorphism with bounded vertex degree (bounded valency of the atoms), however, can be solved in polynomial time [77]. We transform the molecular graphs into their *canonical* SMILES representation [120, 121]. The isomorphism test then reduces to simple string comparison.

[1] from `http://www.daylight.com/smiles/f_smiles.html`: "SMILES originated in the depths of the US government, where humorous names for things are frowned upon unless they are acronyms."

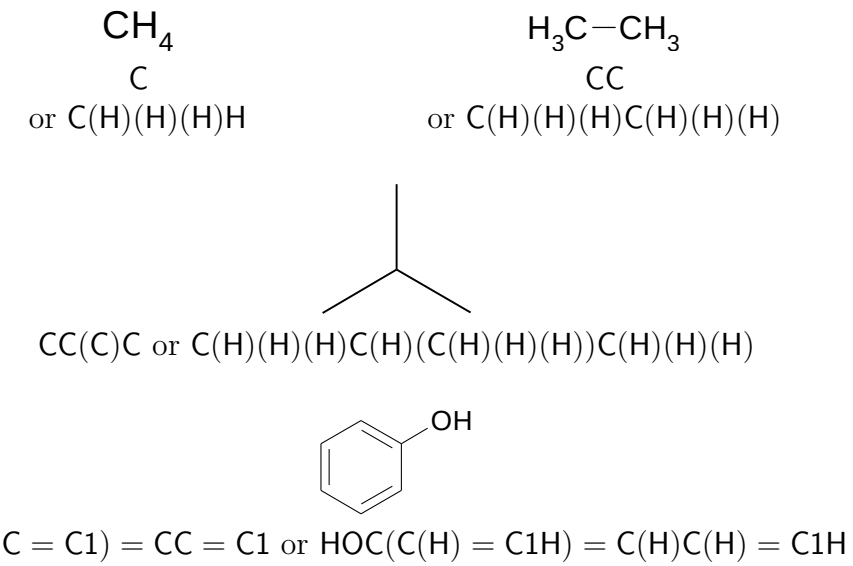

Figure 3.6: An extremely brief SMILES tutorial.

The BNF notation of the subset of SMILES used in the Toy Model is:

```
atom ::=   'C' | 'N' | 'O' | 'H'

bond ::=   <empty> | '-' | '=' | '#'

chain ::=  <atom>
           | <atom> <bond> <chain>

branch ::= '(' <chain> ')'
           | '(' <chain> <branch> ')'
           | '(' <branch> <chain> ')'
           | '(' <chain> <branch> <chain> ')'

smiles ::= <chain>
           | <chain> <branch>
```

In addition to these rules, which describe trees, cycles are indicated by adding identical digits to the atoms closing a cycle. Hydrogen atoms may be included implicitly or explicitly. See fig. 3.6 for a quick list of examples.

The canonical SMILES are built using rules described in [121]. First a graph data structure with canonical labeling and ranking is built, ordered according to the labels and ranks. Then a unique SMILES is generated,

whereby branching decisions in the SMILES tree rely again on the ranking and labeling.

A SMILES uniquetizer is available from `outreach@superior.dul.epa.gov` and `http://www.epa.gov/med/databases/smiles.html`. It transforms SMILES into unique SMILES (USMILES) such that two identical molecules, i.e. with isomorphic graphs, have the same USMILES. The USMILES may serve as a unique identifier, which is needed for the CRN generation (ch. 5). By using USMILES, the graph isomorphism test reduces to a simple string comparison.

A number of other distinct representations of (organic) molecules are used in different programs:

- **IUPAC Nomenclature** is in principle able to give a unique representation of a molecule. IUPAC-names are, however, rather uncomfortable to parse.
  Heptacyclo[7.5.1.0 2,14 .0 5,12 .0 5,15 .0 8,10 .0 11,13]pentadecane

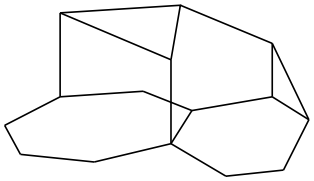

- **WLN WISSWESSER LINE NOTATION** [116] is based on an aggregate representation of the molecule in which symbols represent entire functional groups.

  Example: QVYZ1RDQ is the code for

  $(\mathsf{OH}-)(-\mathsf{CO}-)(-\mathsf{HCNH_2}-)(-\mathsf{CH_2}-)(-\mathsf{C_6H_5})(\mathsf{para})(-\mathsf{OH})$, i.e.:

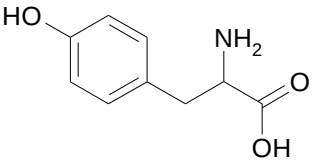

- **Registry Numbers.** Every new organic compound gets an arbitrary number in Chemical Abstracts (CAS) or Beilstein (CCID). Clearly, this representation is not useful for the purpose of generating reaction networks.

- **Fragmentation Codes.** The two main systems are GREMAS (Genealogische Recherche mit Magnetband-Speicherung) [12, 44] and the

Derwent Fragmentation Codes, which are often used in patent search systems. The idea is to subdivide the structure into fragments that are then represented by three-letter codes of the form Genus / Species / Subspecies, e.g. EAD = Alcohol/free alcohol/free aromatic alcohol. This systems is rather complicated, hard to adapt to new chemistries, and very hard if not impossible to convert into a canonical representation.

- **Connection Tables.** A molecule is represented as a list of atoms and a list of bonds connecting these atoms. There is a plethora of file formats. MOL and SDF Files are simple flat format files, and the most used ones, see `http://www.mdli.com/downloads/literature/ctfile.pdf`.

3.4 Wave function analysis

The generalized eigenvalue problem can be transformed into a standard (symmetric) eigenvalue problem using a congruence transformation by factorizing the metric, here overlap matrix [124, sect. 1.31, 5.71]. Because the basis set is orthogonalized, the transformation is called orthogonalization.

In the Toy Model, Löwdin's symmetric orthogonalization with $\mathbf{S} = \mathbf{S}^{1/2}\mathbf{S}^{1/2}$ is used. $\mathbf{S}$ is assumed to be positive-definite (it should be noted that too big overlaps (> 0.8) may lead to a non-positive-definite overlap matrix). Eq. 3.11 then transforms to the symmetric form:

$$(\mathbf{S}^{-1/2}\mathbf{H}\mathbf{S}^{-1/2})\mathbf{C}' = \mathbf{C}'\mathbf{E}\,, \tag{3.14}$$

where $\mathbf{C}' = \mathbf{S}^{1/2}\mathbf{C}$.

Using this method, the overlap matrix stays exactly symmetric and fewer numerical errors than in the canonical method are introduced. In canonical orthogonalization, a Cholesky decomposition $\mathbf{S} = \mathbf{L}\mathbf{L}^T$ is used. This method is more efficient than the calculation of $\mathbf{S}^{-1/2}$ but more error-prone. Numerical errors may also break the symmetry of a molecule. However, there are further developments leading to linear scaling algorithms for those matrix computations [19].

The total electronic energy of the molecule is obtained by the formula

$$E = \sum_i n_i E_i\,, \tag{3.15}$$

where n_i is the occupation number of the MO ϕ_i.

The electron distribution is derived from eq. 3.9 by using a partitioning, e.g. isolating one summand for each atom. The only way of identifying in the

Toy Model to which atom an electron belongs is by the AOs. Furthermore, as Löwdin's method was used for the orthogonalization, it is straightforward to use Löwdin partitioning for population analysis. This is equivalent to performing the partitioning in the orthogonalized basis $\chi' = \mathbf{S}^{1/2}\chi$, where $S'_{jk} = \delta_{jk}$. Summing over all MO, as in eq. 3.15, the total number of electrons N is written as:

$$\begin{aligned} N &= \sum_i n_i \\ &= \sum_i n_i \sum_{j,k \in AO} C'_{ji} C'_{ki} \delta_{jk} \\ &= \sum_i n_i \sum_{j \in AO} C'^2_{ji} . \end{aligned}$$

Using the sum over all $j \in AO$, N can be partitioned such that for an atom A and AOs i on A ($i@a$)

$$\rho_A = \sum_i n_i \sum_{j@A} C'^2_{ji} .$$

The charge on A is then the sum between the nuclear charge and the electronic population: $Q_A = Z_A - \rho_A$.

This population analysis combines well with the choice of a Slater-type orbital basis set. The orbitals describe the wave functions close to the atom they are centered on, thus their LCAO coefficient can describe the electron population on that atom.

As an example, the overlap matrix constructed for propenamide is shown (tab. 3.6). Only the SMILES C=CC(=O)N was needed for its generation and the subsequent calculation of energy levels (fig. 3.8) and charge distribution (fig. 3.7).

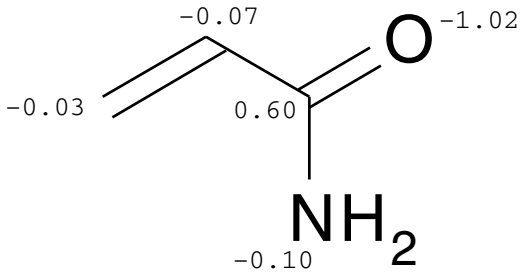

Figure 3.7: Charge distribution in propenamide (in electron charges).

Table 3.6: Overlap matrix for propenamide (fig. 3.5). First and second rows are the atom and the the type of the AO. The indices next to the atom names are given for better orientation and correspond to the indices in the propenamide SMILES $C^1(H^2)(H^3) = C^4(H^5)C^6(=O^7)N^8(H^9)H^{10}$.

C^1	H^2	C^1	H^3	C^1	C^4	C^4	H^5	C^4	C^6	C^6	O^7	C^6	N^8	N^8	H^9	N^8	H^{10}	O^7	O^7	C^1	C^4	C^6	O^7	N^8
sp^2	s	sp^2	s	sp^2	sp^2	sp^2	s	sp^2	sp^2	sp^2	sp^2	sp^2	sp^2	sp^2	s	sp^2	s	sp^2	sp^2	p	p	p	p	p
1	.65	0	0	0	.077	0	0	0	0	0	0	0	0	0	0	0	0	0	0	0	0	0	0	0
.65	1	0	0	0	0	0	0	0	0	0	0	0	0	0	0	0	0	0	0	0	0	0	0	0
0	0	1	.65	0	.077	0	0	0	0	0	0	0	0	0	0	0	0	0	0	0	0	0	0	0
0	0	.65	1	0	0	0	0	0	0	0	0	0	0	0	0	0	0	0	0	0	0	0	0	0
0	0	0	0	1	.77	.077	0	.077	0	0	0	0	0	0	0	0	0	0	0	0	0	0	0	0
.077	0	.077	0	.77	1	0	0	0	.077	0	0	0	0	0	0	0	0	0	0	0	0	0	0	0
0	0	0	0	.077	0	1	.65	0	.077	0	0	0	0	0	0	0	0	0	0	0	0	0	0	0
0	0	0	0	0	0	.65	1	0	0	0	0	0	0	0	0	0	0	0	0	0	0	0	0	0
0	0	0	0	.077	0	0	0	1	.77	.077	0	.077	0	0	0	0	0	0	0	0	0	0	0	0
0	0	0	0	0	.077	.077	0	.77	1	0	.068	0	.073	0	0	0	0	0	0	0	0	0	0	0
0	0	0	0	0	0	0	0	.077	0	1	.68	0	.073	0	0	0	0	.068	.068	0	0	0	0	0
0	0	0	0	0	0	0	0	0	.068	.68	1	.068	0	0	0	0	0	0	0	0	0	0	0	0
0	0	0	0	0	0	0	0	.077	0	0	.068	1	.73	.073	0	.073	0	0	0	0	0	0	0	0
0	0	0	0	0	0	0	0	0	.073	.073	0	.73	1	0	0	0	0	0	0	0	0	0	0	0
0	0	0	0	0	0	0	0	0	0	0	0	.073	0	1	.63	0	0	0	0	0	0	0	0	0
0	0	0	0	0	0	0	0	0	0	0	0	0	0	.63	1	0	0	0	0	0	0	0	0	0
0	0	0	0	0	0	0	0	0	0	0	0	.073	0	0	0	1	.63	0	0	0	0	0	0	0
0	0	0	0	0	0	0	0	0	0	0	0	0	0	0	0	.63	1	0	0	0	0	0	0	0
0	0	0	0	0	0	0	0	0	0	.068	0	0	0	0	0	0	0	1	0	0	0	0	0	0
0	0	0	0	0	0	0	0	0	0	.068	0	0	0	0	0	0	0	0	1	0	0	0	0	0
0	0	0	0	0	0	0	0	0	0	0	0	0	0	0	0	0	0	0	0	1	.38	0	0	0
0	0	0	0	0	0	0	0	0	0	0	0	0	0	0	0	0	0	0	0	.38	1	.38	0	0
0	0	0	0	0	0	0	0	0	0	0	0	0	0	0	0	0	0	0	0	0	.38	1	.26	.31
0	0	0	0	0	0	0	0	0	0	0	0	0	0	0	0	0	0	0	0	0	0	.26	1	0
0	0	0	0	0	0	0	0	0	0	0	0	0	0	0	0	0	0	0	0	0	0	.31	0	1

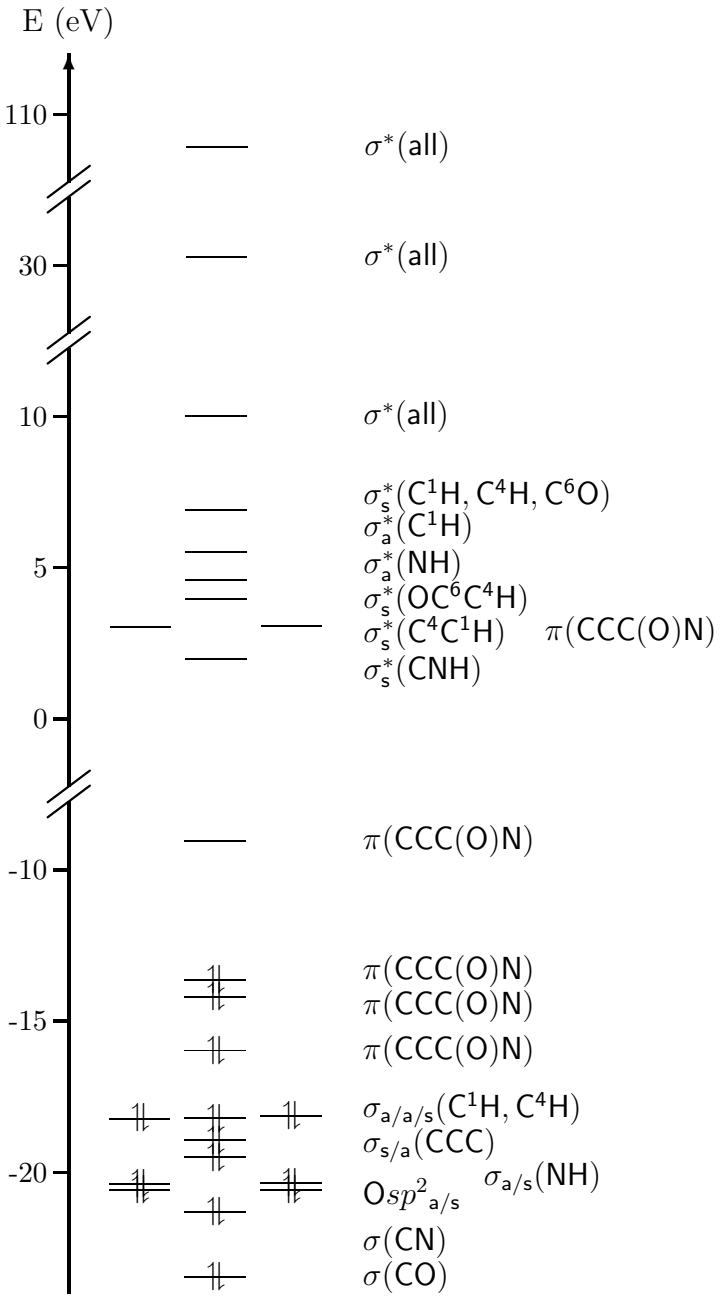

Figure 3.8: Spectrum (MO energies) of propenamide and their types. $\sigma^*_{\mathsf{a}}(\mathsf{NH})$ means that the MO is concentrated on the σ overlap(s) between N and the Hs attached to it. The indices $*$ and a (antisymmetric, as opposed to s, symmetric) indicate that the LCAO coefficients C_{ij} (see sect. 3.1) of the atoms N and H are of opposite sign regarding (Nsp^2,Hs)-pairs ($*$) and of same magnitude but opposite sign regarding (Nsp^2,Nsp^2)- and (Hs,Hs)-pairs (a). The indices on the atoms are the same as in fig. 3.6.

3.5 Performance

In order to validate the energy calculation, predicted total atomization energies (TAE) have been compared to experimental ones, see figs. 3.9 and 3.10. Experimental TAE values are taken from [18].

Fig. 3.9 shows well how every $-\mathsf{CH_2}-$ unit corresponds to an energy increment [11]. The distance between two successive points is almost constant. Indeed, this can be rationalized by the fact that **S** and **H** can be brought into a *quasi*-block-diagonal form, every block corresponding to one $-\mathsf{CH_2}-$ unit. It follows that the total energy is proportional to the number of these units.

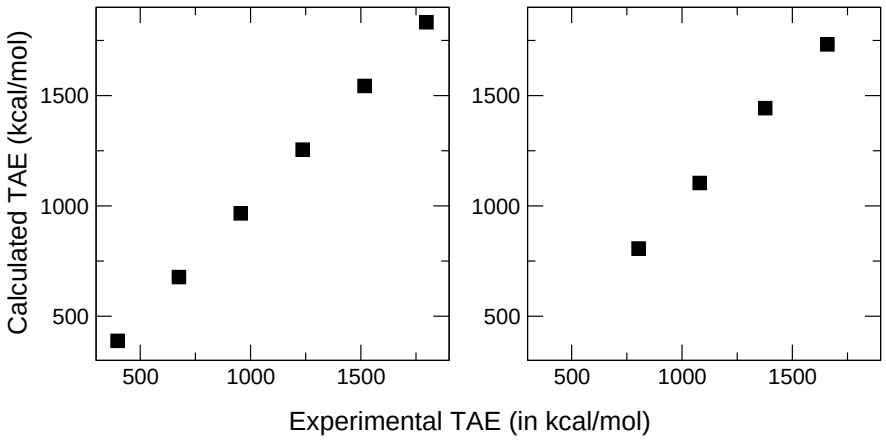

Figure 3.9: Comparison of calculated and experimental Total Atomization Energy (TAE) for homologous series of alkanes (methane to hexane, left) and cycloalkanes (cyclopropane to cyclohexane, right).

Fig. 3.10 shows a reasonable correlation, given the rough approximations of the Toy Model. The same TAE are calculated for cis/trans isomers because their are topologically equivalent (Z,Z- and E,Z- and E,E-2,4-hexadiene, for example). Moreover, a big part of the energy differences between the $\mathsf{C_6H_{10}}$ stems from electrostatic repulsion, which depends on the steric configuration ignored by the Toy Model (see ch. 7 for improvements).

The Toy Model does obviously not include the calculation of vibrational and rotational energy and of entropy. [18, 67] discuss methods for their approximation. However, it seems that their contribution is small.

Highest Occupied MOs (HOMOs) of type σ instead of π are predicted for some olefinic systems. However, this is in agreement with the results of [57, vol. I, fig. 10.33].

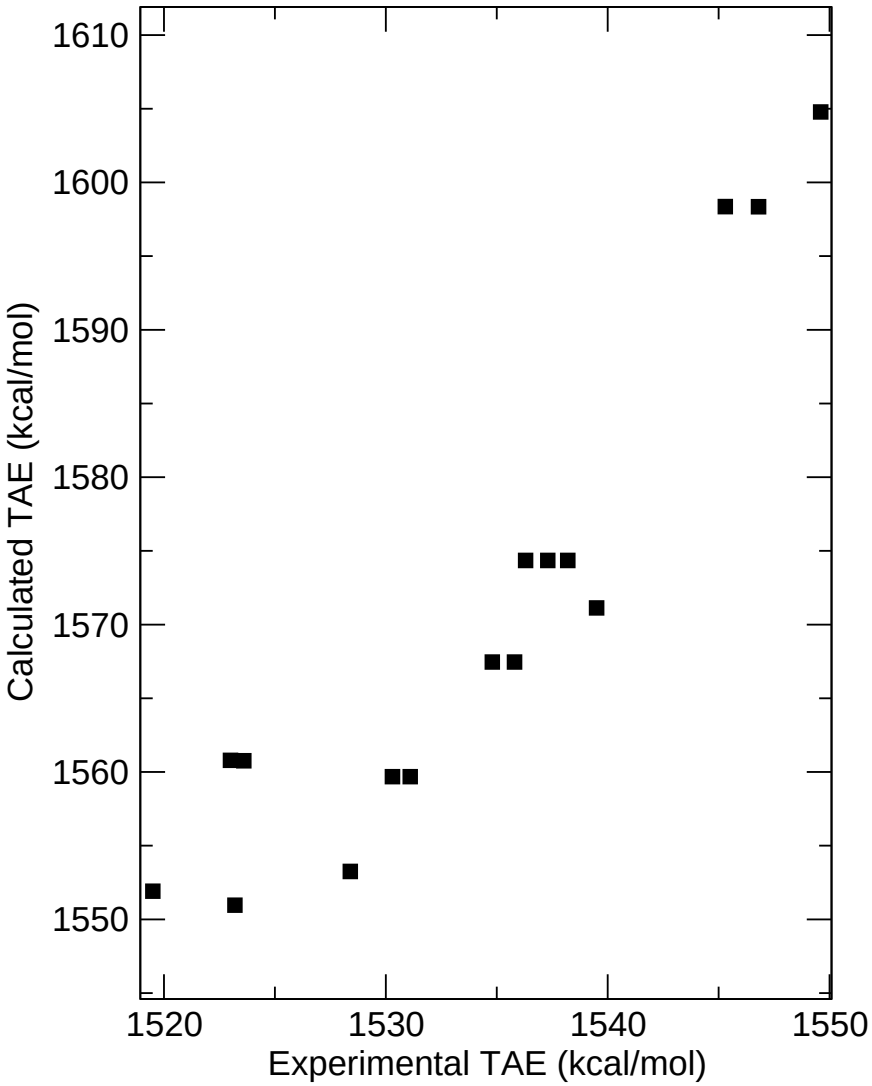

Figure 3.10: Plots of calculated vs. experimental TAE for C_6H_{10} isomers, in order of increasing experimental TAE those are 1-hexyne, 2- and 3-hexyne, 3,3-dimethyl-1-butyne, 1,5-hexadiene, Z- and E-1,4-hexadiene, Z- and E-1,3-hexadiene, Z,Z- and E,Z- and E,E-2,4-hexadiene, bicyclo[3.1.0]hexane, 4- and 3-methylcyclopentene, 1-methylcyclopentene.

3.6 Frontier Molecular Orbital Theory

It is natural to continue with the qualitative theory of Frontier Molecular Orbital (FMO) theory after having used EHT for molecular property calculation. From perturbation theory, the energy increment incurred by the reactants A and B by interacting at the start of a reaction is the Klopman-Salem formula [71, 99]

$$\begin{aligned}\Delta E &= \sum_{a\in A, b\in B} G_{ab} + \sum_{a\in A, b\in B} \frac{q(a)q(b)}{\epsilon r_{ab}} \\ &\quad - \left(\sum_{\alpha\in A}^{\text{occ}} \sum_{\zeta\in B}^{\text{unocc}} F^{\alpha,\zeta} + \sum_{\alpha\in B}^{\text{occ}} \sum_{\zeta\in A}^{\text{unocc}} F^{\alpha,\zeta} \right) \\ G_{ab} &= -\sum_{i@a} \sum_{j@b} (q_i + q_j) H_{ij} S_{ij}\,, \\ F^{\alpha,\zeta} &= \frac{2}{E_\zeta - E_\alpha} \left(\sum_{a\in\mathcal{A}} \sum_{i@a} \sum_{b\in\mathcal{B}} \sum_{j@b} C_{\alpha,i} C_{\zeta,j} H_{ij} \right)^2 ,\end{aligned} \tag{3.16}$$

where r_{ab} is the bond length, ϵ is the dielectric constant of the reaction medium and $\alpha \in$ A and $\zeta \in$ B is an occupied and an unoccupied MO, respectively. This increment is extrapolated in FMO theory from the initial stage of the reaction to the transition state and may thus serve to approximate the reaction rate. It can be derived to predict relative reactivities and regioselectivity as described in [38]. The reactivity is then inversely proportional to the difference of the HOMO and LUMO energies of the reactants. The regioselectivity is determined by the MO coefficients at the reactive sites i, such that $\sum_i C_{HOMO,i} C_{LUMO,i}$ is maximal.

With the abbreviation

$$W_{ab}^{\alpha\zeta} = \sum_{i@a} \sum_{j@b} C_{\alpha,i} C_{\zeta,j} H_{ij} \tag{3.17}$$

we obtain a four-point term

$$F_{ab;a'b'} = 2 \sum_{\alpha\in\mathcal{A}}^{\text{occ}} \sum_{\zeta\in\mathcal{B}}^{\text{unocc}} \frac{W_{ab}^{\alpha\zeta} W_{a'b'}^{\alpha\zeta}}{E_\zeta - E_\alpha} + \sum_{\alpha\in\mathcal{B}}^{\text{occ}} \sum_{\zeta\in\mathcal{A}}^{\text{unocc}} \frac{W_{ba}^{\alpha\zeta} W_{b'a'}^{\alpha\zeta}}{E_\zeta - E_\alpha} \tag{3.18}$$

that allows us to write ΔE as an expansion of atom pairs and quadruples. Within the approximation of the Toy Model all contributions (with the exception of the Coulomb term) that do not belong to new bonds (or bonds

with increasing bond order) vanish because their overlap integrals are zero. Thus

$$\Delta E = \sum_{(a,b)} \left(G_{ab} + \frac{q(a)q(b)}{\epsilon r_{ab}} - F_{ab;ab} \right) - \sum_{(a,b)\neq(a',b')} F_{ab;a'b'} \tag{3.19}$$

where the sums run only over newly formed bonds (a, b). The same formalism can be applied to intra-molecular reactions by setting A = B; in eq. 3.18 we then retain only one of the two double sums (which become identical in this case). The reactivity ΔE allows us to model regioselectivity. If more than one subgraph isomorphism, i.e. more than one possible reaction channel, has been found one simply has to evaluate ΔE for all of them. Then the rewrite with the smallest ΔE value is chosen.

Eq. 3.16 has three terms which allow to classify reactions in three groups [38, 67, ch. 2 resp. ch. 15]. The first term is mainly constant and depends mostly on the *steric* configuration during a reaction. The second term is most important for polar reactants, in *charge controlled* reactions. The third term will dominate for non-polar reactants, in *orbital controlled* reactions. FMO theory only considers the last term. Although its numerical contribution is small, this approach is justified by the fact that the shapes of the HOMO and LUMO resemble to the total electron density important for the reactivity. Keeping in mind that MOs do not exist in reality, they are still constructs of MO thoery useful for explaining energy differences between "real" electronic states.

The situation can be simplified further by considering only the frontier orbitals [46], i.e. the HOMO of one system and the LUMO of the other one. In this case the sums in eq. 3.18 reduce to a single term. Often this is approximated by $\Delta E^{\ddagger} = \xi/(E_{\zeta} - E_{\alpha})$ with an empirical constant ξ that depends only on the reaction mechanism [38]. The reaction rate and activation energy are related by Arrhenius' law $\Delta E^{\ddagger} = RT \ln k$. The regioselectivity is determined by the MO coefficients at the reactive sites, such that $\sum_i C_{HOMO,i} C_{LUMO,i}$ is maximal. This simplification was used for generating the two examples in chapter 6, figs. 6.1 and 6.2.

Chapter 4

Chemical reactions

> A molecule is composed of atoms that are tied together by aid of the electrons. Atomic nuclei and electrons are not at rest but are constantly moving. The paths of the electrons are usually called orbitals. The forms of these orbitals are determining the bonds between the atoms. In a reaction molecules are impinging against each other. During the collision the electrons are influenced by new atomic nuclei and the orbitals are changed. Some of the bonds are broken and others are created. Afterwards, new molecules have been formed.
>
> The Nobel Prize in Chemistry 1981. Presentation Speech by Professor Inga Fischer-Hjalmars of the Swedish Royal Academy of Sciences

4.1 Graph rewriting

This section summarizes the work of Dörr [29] and [37] and explains how it can be applied to the problem of implementing chemical reactions.

As we represented molecules as graphs, it is natural to simulate the set of reactions by *generic reactions* (see sect. 2.2) in the framework of a *graph grammar* [82, 97]. A graph grammar is a finite set of rules operating on edge and vertex labeled graphs. The term "graph grammar" is rather used for graph-generating applications. In our context, the similar term "graph rewriting system" used for graph-transforming application is more appropriate.

Graph transformations have been studied first 30 years ago [84] for the generation, manipulation, recognition of graphs. Four types of applications

exists: the aforementioned graph grammar, unordered, ordered, and event-driven graph rewriting systems. The first uses a set of rules, a host graph, and terminal (ending) labels to generate a language or for parsing. The second consists only of a set rules and rewrites a graph without further considerations. The third and fourth type include specifications controlling the rewriting, for example when to stop. The Toy Model uses the event-driven type, where the sequence of rewritings/reactions is controlled from outside, depending on other (energy) calculations.

Graph rewriting systems have been applied to a variety of domains. Pattern recognition and specification of database systems are easily conceivable uses, but also less obvious approaches are possible. Visual languages might be defined using graph transformation, and relatedly, also the semantics of other languages or compilers. With the project PARES [97, ch. 12] there is even an example for the application of graph grammars to art. In PARES, the paintings of Picasso[1] are reconstructed, starting with an empty canvas, and using derivation rules. Each rule adds new structural information, until a typical cubist painting is obtained.

A major problem in graph rewriting is the complexity of subgraph isomorphism. A subgraph $h = (V_h, E_h)$ of a graph g is defined by $V_h \in V_g$ and $E_h \in V_h \times V_h$. An isomorphism is defined on two graphs g_1 and g_2 as the bijective application $f : V_1 \to V_2$ such that $(u, v) \in E_1 \iff (f(u), f(v)) \in E_2$. The subgraph isomorphism problem is NP-complete [49] (for the graph isomorphism problem, it is not known whether it is NP-complete). Theoretical investigations have shown that there exists a moderately exponential bound for the general problem [7]. More practical approaches have started with backtracking [22], refined by reducing the search space, as reviewed by [97].

Dörr describes an algorithm in which breadth-first-search determines all subgraphs isomorphic to the rewrite rule left-hand side. The search is implemented as an abstract machine, i.e. a software implementation of a processor, including an instruction set, a register set, and a model of memory. For a faster implementation, only one abstract machine for all host graphs is generated. Furthermore, a search strategy adapted to a subclass of graphs rewriting systems is adopted to obtain an efficient solution, in contrast to the general NP-complete problem. The search uses a sufficient condition for which the algorithm performs in constant time. The condition is based on graph properties of the graph rewriting system (sets of unique vertex labels and strong V-structures). A rewriting system for which all rules satisfy the condition is called *Unique vertex label and Bypassing Strong V-structures* (UBS) .

[1] "Computers are useless. They can only give you answers." – Pablo Picasso

Graphical transformations can be described in terms of graphical pre- and post-conditions. It is possible to use a rule-based notation for this transformation. Such a rewrite rule is a tuple $r = (g_l, g_r, M)$, where the graph g_l is the left-hand side, g_r is the right-hand side, and M is the set of embedding descriptions (important for the dangling ends). The implementation used in the Toy Model defines g_l and g_r by the elements of the graph no longer and only present after the transformation, respectively, and by a context which contains the constant element, see figs. 4.1 and 4.2.

The execution of the rewrite rule is decomposed into four steps:

- find an isomorphic subgraph (to g_l)
- remove that subgraph (keeping the dangling ends in M)
- insert a new subgraph (g_r)
- connect it to the rest of the graph (respecting the dangling ends from M)

This graph rewriting formalism is very flexible and can be used to represent chemical reactions as well as chemically impossible yet strategically interesting reactions. It may be interesting to use scaffold replacement rules for building a library in combinatorial chemistry, or to simulate deprotonation implicitly, but in reality, chemical reactions do not create or destroy atoms. A chemical reaction is the breaking, forming and changing of bonds. Thus the number and type of atoms must remain constant, which can be implemented by *conservation of vertex labels*. In analogy, the conservation of the number of valence electrons can be imposed on rewrite rules by ensuring *conservation of total bond order*. Both principles stem from the fact that chemical reactions are stoichiometric [31, 113]:

- *conservation of vertex labels* : $V_l = V_r$
- *conservation of total bond order* : $\sum_{e \in E_l} BO(e) = \sum_{e \in E_r} BO(e)$,

where V_i and E_i are the vertices and the edges of g_i, and $BO(e)$ is the bond order of the edge e . In the example of the Diels-Alder reaction in fig. 4.2, the first condition is met because all atoms are in the constant set, the context. Counting the bond orders of g_l (2+2+1+2) and g_r (1+1+1+2+1+1) verifies that the second condition is also satisfied, thus this rewrite rule is chemically meaningful.

This reaction representation has the advantage of representing the reaction itself also by graphs, and thus does not have the inherent limitations

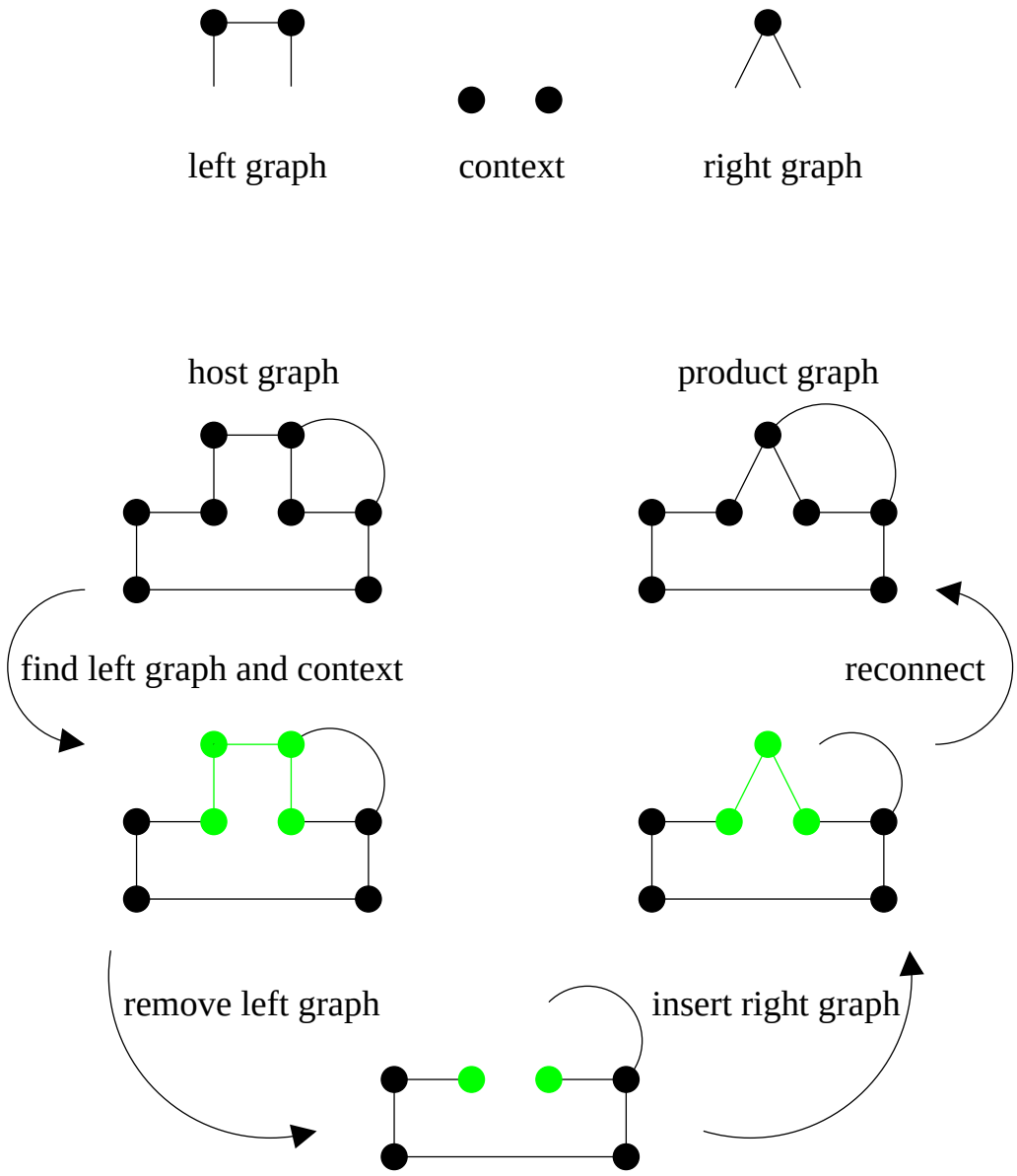

Figure 4.1: Graph rewriting steps.

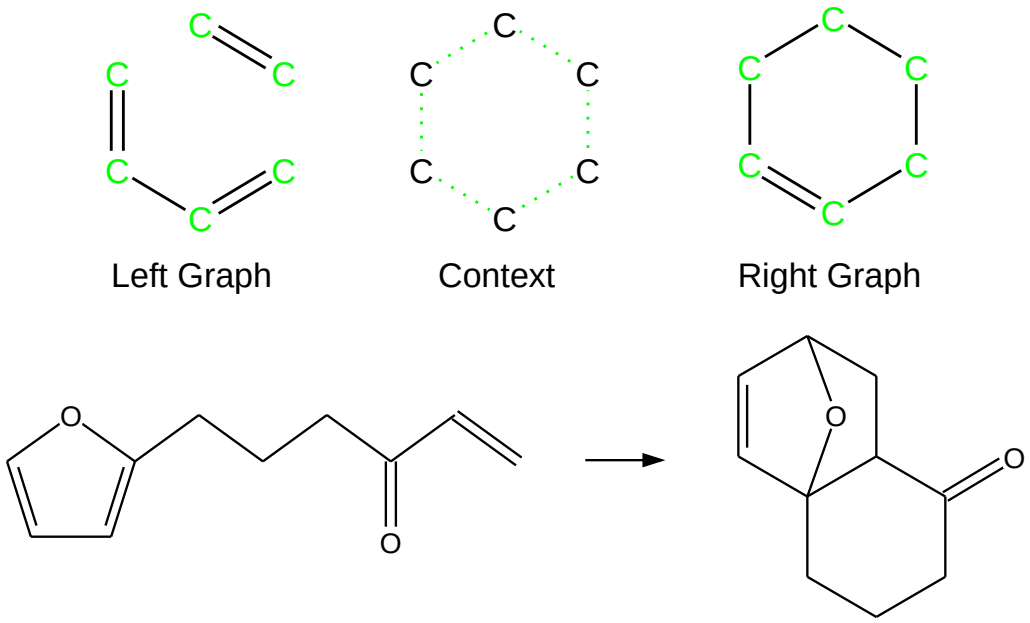

Figure 4.2: Intramolecular Diels Alder rearrangement (iDAR). Top: rewrite rule; since all bounds change their type during the rewrite, the context consists of the six C-atoms only. Bottom: Application of iDAR to the synthesis of a bridged ring system.

of string representations, for example. It is also, of course, more flexible and simpler than a hard-coded implementation of reactions, as complicated reactions might be very time-consuming to encode one per one.

4.2 Graph Rewrite Engine

Dörr's algorithm uses connected enumeration, i.e. g_l must be connected. Thus for every pair of vertices $(u, v) \in V \times V$ there must be a list of vertices $(v_1 \dots v_n)$ with $v_i \in V$, such that all pairs (v_i, v_{i+1}) are connected by an edge. Yet a rewrite rule corresponding to a bimolecular reactions will have a disconnected g_l, composed by two subgraphs corresponding to the two reacting entities. The two subgraphs can not be connected by an edge, as the two molecules are not bonded prior to reaction.

In the Toy Model, reactions are simulated by a separate Graph Rewrite Engine (GRW). The GRW simulation of unimolecular reactions is a straight forward application of rewrite rules to a molecule. A bimolecular reaction or any other similar rule is split by the GRW into one half reaction rule for each educt molecule, and a final reaction rule. The two half reaction rules do not modify existing bonds and atoms in the molecules, they just add "flag" nodes to the atoms that will be joined during the total reaction. They serve to identify those reaction sites for the reactivity evaluation in sect. 3.6. The evaluation determines which pairs of reaction sites from each of the two reactants are joined by a temporary edge. This temporary construct is then again submitted to the final reaction rule and transformed to the product. Fig. 4.3 shows the reaction rules of the aldol reaction.

There are bimolecular reactions like Cannizzaro's disproportionation [16], olefin metathesis [127] or organic catalysis whence two products emerge. As g_r need not be connected, the final reaction rule can be adapted to this situation.

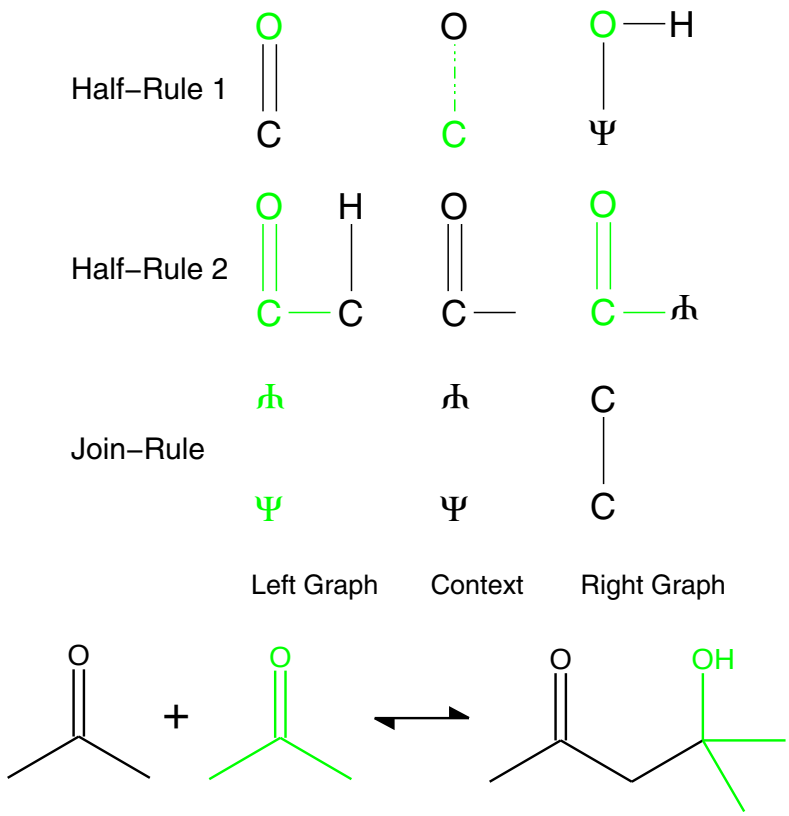

Figure 4.3: Aldol Reaction. Top: rewrite rule; the two half-rules describe the local changes in the reacting molecules during Aldol condensation, while the half-rule-join describes only intermolecular changes; notice the special label Ψ, acting as anchor for the intermolecular bond to be formed. Only the elements in black are actually contained in the rules, the other elements are displayed to hint at their embeddings. Bottom: Application to the synthesis of β-hydroxy-carbonyls.

Chapter 5

Reaction networks

5.1 Network generation

The starting point for generation a CRN is an initial set of molecules $\mathfrak{L}_0$. At the present stage of development, the CRN is built exhaustively from the network "seed" $\mathfrak{L}_0$. The algorithm used can be termed "orderly generation" for its resemblance to an algorithm of this name used for enumeration of isomers [93, 33]. It generates the CRN by the following recursion:

Start **(1)** perform all unimolecular reactions on each molecule $\mathrm{M} \in \mathfrak{L}_0$ and put the products in a new set $\mathfrak{L}_1'$, eliminating all duplicates.

(2) perform all bimolecular reactions with each pair of molecules $(\mathrm{M}_1, \mathrm{M}_2) \in \mathfrak{L}_0 \times \mathfrak{L}_0$ and add the products to set $\mathfrak{L}_1'$, eliminating again all duplicates. The last two steps are summarized by the notation $\mathfrak{L}_1' = \mathfrak{L}_0 \otimes \mathfrak{L}_0$. $\mathfrak{L}_i \otimes \mathfrak{L}_j$ means that step 1 is applied only to the first operand $\mathfrak{L}_i$, and step 2 on pairs $(\mathrm{M}_1, \mathrm{M}_2) \in \mathfrak{L}_i \times \mathfrak{L}_j$.

(3) this first iteration is completed by calculating $\mathfrak{L}_1 = \mathfrak{L}_1' \setminus \mathfrak{L}_0$.

Recursion **(1)** $\mathfrak{L}_{k+1}' = \left(\bigcup_{j=0}^{k-1} \mathfrak{L}_j\right) \otimes \mathfrak{L}_k \cup (\mathfrak{L}_k \otimes \mathfrak{L}_k)$

(2) and $\mathfrak{L}_{k+1} = \mathfrak{L}_{k+1}' \setminus \bigcup \mathfrak{L}_k$.

Let us now consider the rewriting step for a bimolecular reaction in detail. First the Toy Model sends the two educt graphs to the GRW. The server then constructs all subgraph isomorphisms for the left hand side of both half-rules for both graphs. If the list of subgraph isomorphisms for one of the two half-rules is empty for both graphs, the rule is not applicable and the server sends the two graphs unaltered back to the Toy Model. This case

corresponds to an "elastic collision". Otherwise the server picks a half-rule at random for the first graph and then a corresponding half-rule for the second graph. This corresponds to choosing a reaction channel if there is more than one subgraph isomorphism. Instead of picking a subgraph isomorphism at random from the list, it is possible to consider all reaction channels and to compute a reactivity index for each of them. The Toy Model can then pick the reaction channel (pair of subgraph isomorphisms for the two half-rules). The procedure for a unimolecular reaction is straightforward: the Toy Model sends one molecule to GRW for which in analogy to the previous description all subgraph isomorphism are constructed, and unless there is none, one isomorphism is picked according to its reactivity.

Using the aforementioned algorithm, the CRN is likely to grow very fast. This corresponds for example to the very complex network of elementary reactions constituting a polymerization. The repetitive Diels-Alder networks in fig. 6.1 suffers from this problem. However, there are techniques to simplify such a network called *model reduction* techniques [43]. Reactions may be removed from the CRN during or after generation, or formally "lumped" together before, on the basis of e.g. energetic criteria. It is particularly efficient to perform CRN generation and reduction simultaneously [33, 43], as uninteresting reactions generate products that may further undergo uninteresting reactions and so on. *Detailed* model reduction eliminates such reactions before they can develop further. In the Toy Model, detailed reduction is performed by selecting reactions according to their enthalpy, their activation energy, or both.

5.2 Representation

A chemical reaction network (CRN) is a set of molecules linked together by reactions leading from one subset to another.

A chemical reaction

$$a\mathrm{A} + b\mathrm{B} + \cdots \rightarrow v\mathrm{V} + w\mathrm{W} + \cdots \tag{5.1}$$

can be described as a directed hypergraph [131]. A hypergraph $\mathcal{H}(V, E)$ is a set of vertices and a set of hyperedges, where vertices are elements v_i and hyperedges are pairs of lists of vertices $(\{u_i\}, \{v_i\})$ with $u_i \in \prod V$ and $v_i \in \prod V$ defining connected vertices. The term directed specifies that the order of vertices in the definition of an edge or a hyperedge is important. The chemical species are the vertices. A reaction forms a hyperedge $\boldsymbol{\rho} \in E$ that connects educts with products. A CRN is then represented by a hypergraph with hyperedges for each reaction.

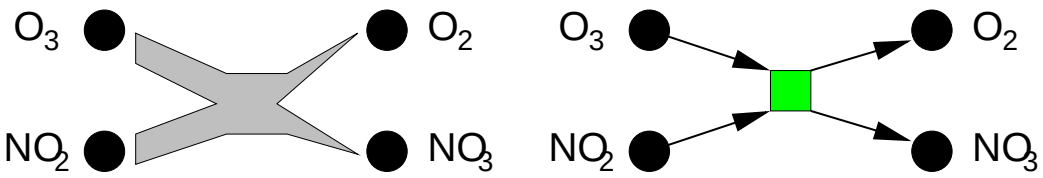

Figure 5.1: Representation of a chemical reaction $\mathsf{NO_2} + \mathsf{O_3} \rightarrow \mathsf{NO_3} + \mathsf{O_2}$ as a directed hypergraph $\mathcal{H}(V, E)$. The chemical species are the vertices $\mathrm{X} \in V$. Each reaction is represented by a single directed hyperedge connecting educts with products. Directed hypergraphs are conveniently displayed as bipartite directed graphs. Here the reactions are represented as a second type of vertices. Directed edges connect educts with the reaction vertex and the reaction vertex with products of the reaction.

Alternatively, a CRN can be described as a bipartite directed graph [9, 132, sect. 2.3.2]. A bipartite graph $\mathcal{V}(V, E)$ can be partitioned into two sets of vertices V_1 and V_2 satisfying $V = V_1 \cup V_2$ and $V_1 \cap V_2 = \emptyset$, such that there is no edge $e = (u, v)$ with $u \in V_1$ and $v \in V_2$. In the bipartite directed graph, molecules are represented by a class of *species vertices*, V_1, and the reactions form a second class V_2 of vertices, *reaction vertices*. Directed edges then connect the educt vertices with the reaction vertex and the reaction vertex with the product vertices, as in fig. 5.1.

5.3 Network properties

It is finally possible to extract properties of the generated CRNs. Ref. [1] reviews interesting graph-theoretic properties of networks. Most of the research is concentrated on the degree distribution, the small-world phenomenon, and the cliquishness in networks. In sect. 6.3, small-world and scale-free networks are described. Both network types may be combined with special cycle distributions, for example an abundance of short cycles [55].

The following characteristics are needed (n and m are the number of nodes and edges) :

- $\langle k \rangle = 2\,\frac{m}{n}$, the average node degree,
- $\langle L \rangle$, the average length of the shortest path between to nodes, and
- $\langle C \rangle$, where $C_i = 2\,\frac{\text{edges between i-neighbors}}{\text{i-neighbors(i-neighbors}-1)}$ is the clustering coefficient. It describes how much the neighborhood of a node resembles to a complete graph, the cliquishness.

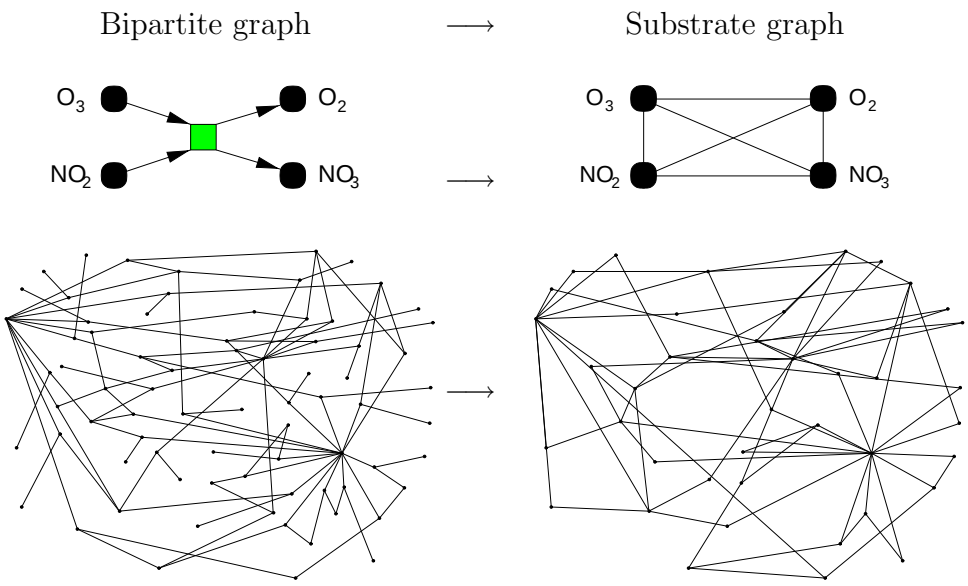

Figure 5.2: One-mode projection from a bipartite graph to a substrate graph.

However, $\langle C \rangle$ is obviously not defined in a bipartite graph. Thus a different representation from the one in figs. 5.1, 6.1 and 6.2 has to be used. The substrate graph [36] is appropriate and obtained from the bipartite graph representation by a one-mode projection (fig. 5.2, [117]). In the substrate graph, all molecules occurring together in a reaction are connected by an edge. It has to be noted that information is lost by projection. The substrate graph is undirected, because elements downstream a reaction pathway may affect elements upstream. For example, even in irreversible reactions, product concentration can affect the reaction rate.

An algebraic representation of a CRN is the *stoichiometric matrix* [132]. In a stoichiometric matrix $\mathbf{N}$, columns correspond to reactions and rows to species. The entry N_{ij} is the *stoichiometric coefficient*, i.e. the number of molecules of i participating in the reaction j. The coefficient is positive or negative depending on whether the species is produced or consumed in the reaction. Reversible reactions are considered as two separate symmetric reactions in opposing directions. Although reactions containing the same species on both sides can be represented by a hyperedge in hypergraph or a cycle of length 2 in a bipartite graph, there is no appropriate stoichiometric coefficient. Nevertheless, reactions of this type, like autocatalytic reactions, can be decomposed into tractable elementary steps, which often corresponds to reality. The stoichiometric matrix is the starting point for control analysis and flux analysis. The program METATOOL [102] derives elementary modes

(see ch. 1) from networks representing metabolic pathways, in which the reactions are controlled by implicit enzymes.

Chapter 6

Computational results

When the three components molecules, reactions, and network simulation are put together, it is possible to build a CRN performing molecular property prediction and model reduction on the fly, given only a list of initial SMILES. For the following CRNs, regioselectivity was simulated using the simple equations described at the end of section 3.6.

6.1 Repetitive Diels-Alder reactions

The Diels-Alder reaction [25] has been extensively studied thanks to its importance in natural products synthesis and because it is easily tractable by simple semi-empirical methods. It is the typical test reaction for a semi-empirical quantum calculation methods such as ours, and furthermore for the numerous approaches of reaction description [110]. It involves the reaction between two linear π-systems of length 2 and 4, called *dienophiles* and *dienes*, and is thus called a [2+4]-cycloaddition. The product is again a dienophile and may react again in a Diels-Alder reaction, then termed *repetitive*. Indeed, the reaction is used for the synthesis of polymers [80]. The CRN in fig. 6.1 is obtained by repetitive Diels-Alder reactions of a simple initial mixture of dienes and dienophiles.

The rewrite rule is a bimolecular variant of the one described in fig. 4.2 (see appendix B). The simple constraints derived from FMO lead to a reaction respecting the Woodward-Hoffmann rules [126]. Depending on which choice makes $|\Delta E_{FMO}|$ smaller, the HOMO of the diene or dienophile reacts with the LUMO of the complementary species. The orientation of the reactants to each other is determined by the FMO coefficients. Model reduction consisted in producing only one of regioisomers instead of both. A further reduction was introduced by an enthalpy threshold of 20 eV.

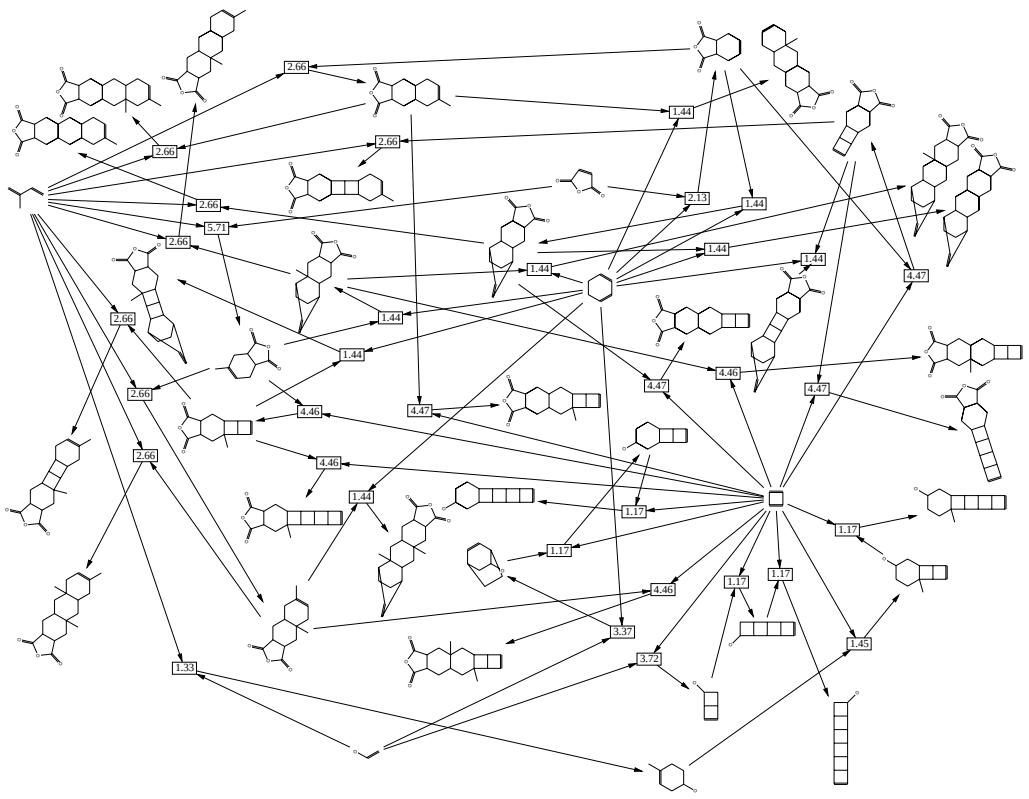

Figure 6.1: Network of Diels-Alder reaction constructed with 3 iterations of the orderly generation algorithm. The initial mixture consists of cyclobutadiene, ethenol, phtalic anhydride, methylbutadiene, and cyclohexa-1,3-diene. Each rectangle represents one reaction, its label indicates the reaction rate using the proportionality constant ξ from [101]. The correlation used is $\Delta E^{\ddagger} = 200/\Delta E_{FMO} - 30$.

6.2 The formose reaction

The synthesis of sugars from formaldehyde under alkaline conditions ("formose reaction") was discovered more than a century ago [15]. It is one of the earliest examples of a reaction network that is collectively autocatalytic in the sense that the reaction products catalyze their own formation. The condensation of formaldehyde proceeds by means of repeated aldol condensations and subsequent dismutations [13, 85]. The formose reaction has been studied in much detail because of its importance as a potential prebiotic pathway [47]. Formaldehyde has been found in the reaction mixture of abiogenesis experiments, right from the start in Miller-Urey's Electric Discharge

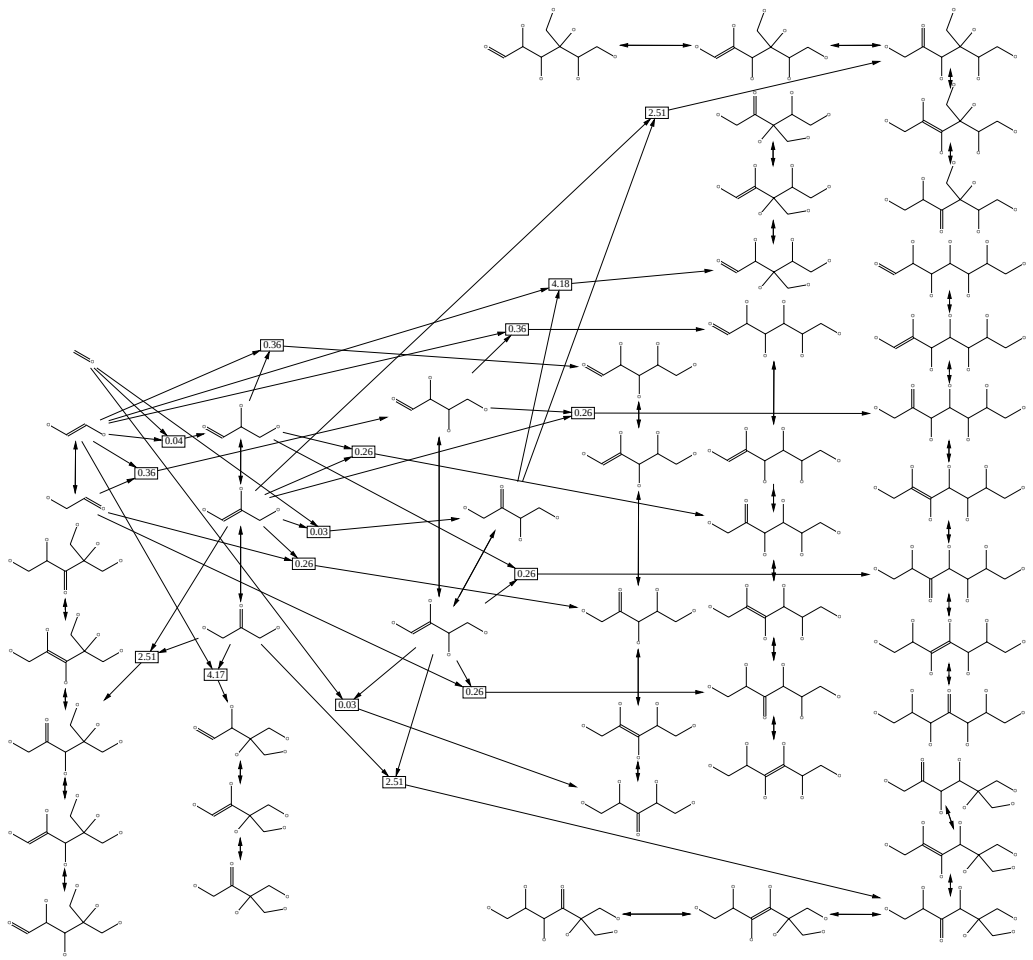

Figure 6.2: Formaldehyde condensation reaction network. The initial mixture consists of formaldehyde $\mathsf{H_2CO}$ and glycol aldehyde $\mathsf{CH_2OH-CHO}$ and reacts via aldol condensations and dismutations. The aldol condensation was simulated by the condensation of a keto with an enole group. In order to account for cyclization, which limits the network, we do not permit carbon chains with more than four members to undergo further aldol condensations. The network generation algorithm thus converges already after two iterations. Reaction rates are computed using the proportionality constant ξ for nucleophilic substitution from [71]. The correlation used is $\Delta E^{\ddagger} = 28/\Delta E_{FMO} - 10\,.$

Experiment [115]. It is thus conceivable that the formose reaction is the origin of biological sugars.

The network produced by the Toy Model is shown in Fig. 6.2. It is built

from a mixture of formaldehyde and glycol. The first condensation step yielding glycol from formaldehyde is assumed implicitly. The rewrite rule used is a variant of the one described in fig. 4.3. In order to account for cyclization, and so to reduce the network, carbon chains with more than four members, or two chains with four members were not permitted to further undergo aldol condensation. Furthermore, although more than 40 different sugars have been identified in the experimental reaction mixture [24], condensation was restricted to enoles with a primary acid hydrogen. Due to this model reduction, the algorithm converged after only two iterations. The Toy Model could be made more accurate by a Monte Carlo CRN generation. It would have the same limits implicitly because unimolecular cyclization is by far faster than bimolecular aldol condensation. This is equivalent to the systematic model reduction described by [43].

6.3 Graph-theoretic properties

For assessing $\langle L \rangle$ and $\langle C \rangle$, we need to compare them to the results for random Erdös-Renyi graphs:

$$\begin{aligned} \langle L_{rand} \rangle &\approx \frac{\ln n}{\ln \langle k \rangle} \\ \langle C_{rand} \rangle &= \frac{\langle k \rangle}{(n-1)} \end{aligned}$$

Tab. 6.1 compares the network characteristics of the Diels-Alder, the Formose, and the *E. coli* metabolic network. They are all sparse graphs, i.e. they have much fewer edges than complete graphs, reflected by $m \ll \frac{n(n-1)}{2}$ or $\langle k \rangle \ll n$. Sparse networks are very common, ranging from the network of acquaintances to a neural network. In both cases, there are only few connections at each node.

The small-world phenomenon [118, 119] is also widespread, and applies for instance to the network of acquaintances. In the latter example, it describes the fact that every person is acquainted to another over "six degrees of separation", in average. More generally, it means that the average shortest path between two nodes in a network is small. An important application is the propagation of diseases, where the small-world property leads to a rapid spread. From the networks of tab. 6.1, only Diels-Alder and *E. coli* fulfill the conditions $\langle C \rangle \gg \langle C_{rand} \rangle$ and $\langle L \rangle \leq \langle L_{rand} \rangle$ and thus are strictly small-world networks. The Formose reaction network includes many non-reactive species with respect to keto-enol condensation, which leads to small cliquishness and longer paths.

Table 6.1: Characteristics of the two example CRNs and the substrate graph of the *E. coli* energy and biosynthesis metabolism [36].

	nodes	$\langle k \rangle$	$\langle L \rangle$	$\langle L_{rand} \rangle$	$\langle C \rangle$	$\langle C_{rand} \rangle$
Formose	48	3.25	3.55	3.28	0.15	0.068
Diels-Alder	40	4.65	2.15	2.40	0.72	0.11
E. coli	282	7.35	2.9	3.04	0.32	0.026

Finally, the degree distributions have been calculated (fig. 6.3). Both networks are scale-free, i.e. their degree distributions follow a power law. The cumulative representation of fig. 6.3 is equivalent to $\int_k^\infty P(x)\mathrm{d}x$ vs. k. The regression $\int_k^\infty P(x)\mathrm{d}x \sim k^{-1.19}$ is consistent with the values reported in [10]. The explanation of the origin of scale-freeness therein can be applied to the present examples. It relies on two generic mechanisms. First, the networks grows from on an initial set of nodes by continuous addition of new nodes. Indeed, in the present case, there is an initial list of molecules, and the networks is built by adding molecules at every iteration (sect. 5.1). Second, the networks grows by *preferential attachment*, i.e. new nodes are preferably attached to nodes with high degree, or in the case of molecules, species who have already spawned many new other species are especially reactive and more likely to produce new molecules at each iteration. The power-law regression for the Formose reaction network fails for high k. The theoretical Poisson distribution for random graphs with high n, $P(k) = e^{-\langle k \rangle} \frac{\langle k \rangle^k}{k!}$, also fails in this range. A degree distribution following a truncated power law has been referred to as *broad-scale* [3].

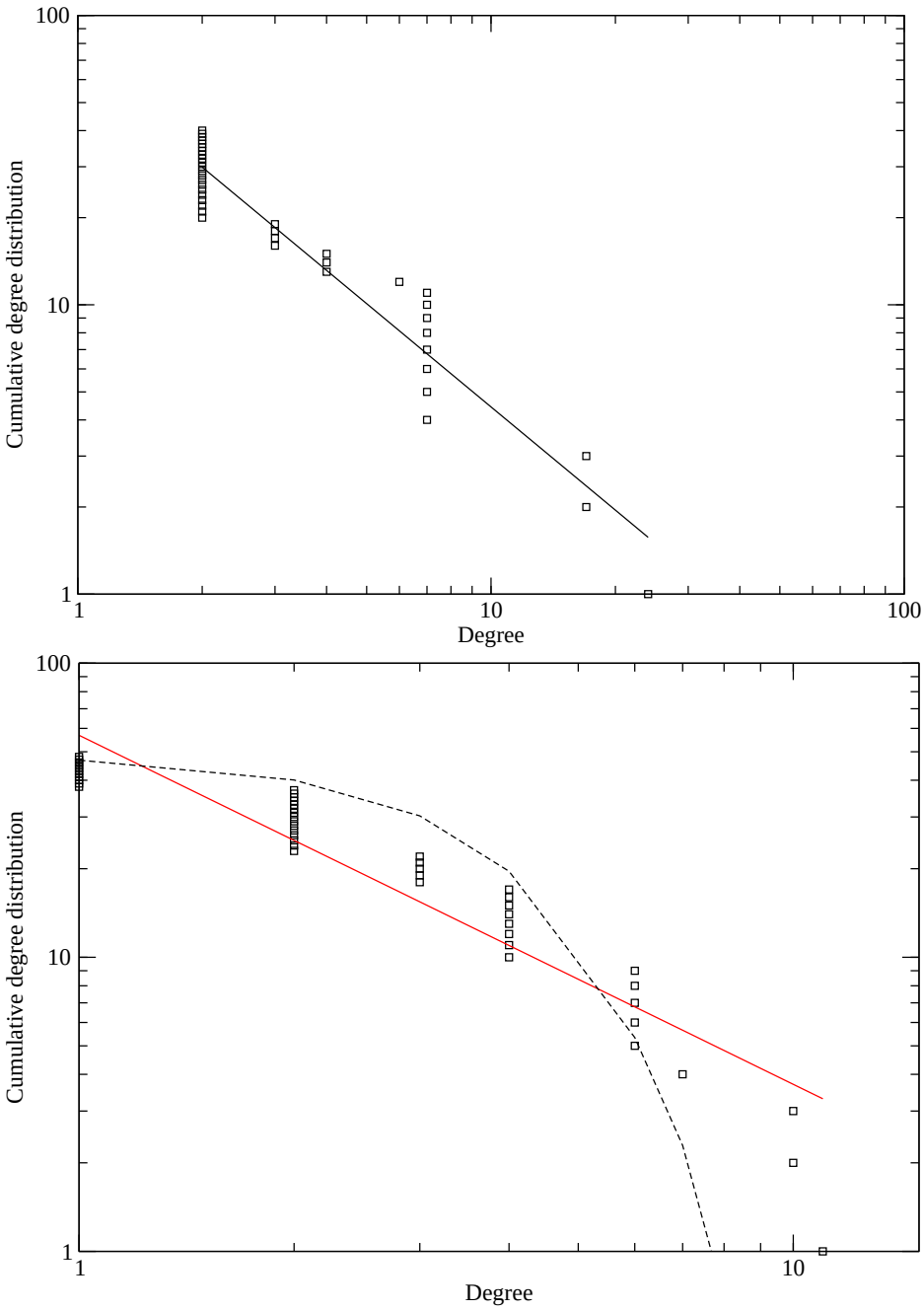

Figure 6.3: Cumulative degree distribution of repetitive Diels-Alder (top) and the Formose reaction network (bottom). Datapoints are ranked by decreasing degree. Datapoints, power-law regressions, and theoretical Poisson distribution are represented by □, solid, and dashed lines. Regressions: $y = 68x^{-1.19}$ with $r^2 = 0.92$ (top), $y = 57x^{-1.19}$ with $r^2 = 0.87$ (bottom).

Chapter 7

Conclusion and Outlook

The present Toy Model is at least close to a minimal implementation of an artificial chemistry exhibiting what we consider the defining features of "real" chemistry. Molecules were represented only by their connectivity information and atom types, as labeled graphs, and their energy was defined along the lines of quantum chemistry, using an extremely simplified function. This energy model forms the basis of full-fledged chemical thermodynamics and kinetics. Chemical reactions are implemented as graph rewriting rules that have to obey the principle of conservation of matter. These features distinguish the Toy Model from artificial chemistries that are defined on abstract algebraic structures such as the λ calculus, Turing machines, or term rewriting. The application of the model to examples of complex organic and prebiotic chemistry allowed an quasi-*ab initio* simulation of the resulting networks and prediction of their properties. Now the emergence of generic properties of CRNs can be studied given only starting material, generic reactions and atom and bond parameters. A true *ab initio* simulation would not need the introduction the latter parameters for the energy calculation and would simulate reactions without even specifying generic reactions. Yet both "educated guesses" are founded on the results of quantum chemistry and synthetic chemistry, and their validity could be estimated by the judicious comparison of predicted to experimental results.

A number of extensions of the present Toy Model are desirable. For instance, the addition of the corresponding parameters (see appendix A) would extend the current implementation of the model, considering only molecules composed of C, H, O, and N, to an expanded set of chemical elements, most importantly S, P, Si, and the halogens. The inclusion of charged particles and radicals also does not seem to pose problems in the current framework. Charges situated on specific atoms can be indicated in SMILES, e.g. HC([O−]) = O. In fact, it does not matter to which atom the

charge is attributed at the beginning, the correct charge distribution is a by-product of the energy calculation (see sect. 3.4). Additional types of chemical bonds, in particular hydrogen bonds and the "three center bonds" common in boron compounds can be approximated by the orbital graph formalism (for boranes, a common object of MO study, see [54, 63, 70]).

The interaction of a molecule with a more complex environment, in particular a solvent, is easily incorporated into the Toy Model using an implicit solvation model [23] such as Kirkwood's equation

$$\Delta G_{\text{solv}} = -\frac{\epsilon - 1}{2\epsilon + 1} \frac{\boldsymbol{\mu}^2}{a^3} \,. \tag{7.1}$$

Here a is the radius of the molecule and $\boldsymbol{\mu}$ is its dipole moment and ϵ is the dielectric constant of the medium. Both a and $\boldsymbol{\mu}$ have to be replaced by appropriate graph descriptors. For example a could be replaced by the Wiener index [56, 123], with a proper normalization. A topological index for vertex weighted graphs could serve as a "graph theoretical dipole moment".

The reactivities from eq. 3.16 can be translated into reaction rate constants, e.g. using Arrhenius' law. An alternative approach to determining rate constants is QSPR [33]. This class of models is, however, of limited interest for our purposes because it is restricted to reaction mechanism for which a sufficient amount of experimental data is available. This method would involve the calculation of descriptors. For steric descriptors, like the aforementioned dipole moment, e.g. graph-theoretic approximations have to be used. In connection to this, an interesting application of the Toy Model would be QSMR for the prediction of CRNs built during the metabolization of a xenobiotic [32]. However, this would require that g_l in the rewrite rule also incorporates descriptors.

The reaction scheme from sect. 4.2 could be modified to select a reaction channel with a probability proportional to its Boltzmann weight $e^{-\Delta E/RT}$, i.e. according to Arrhenius' law. This would be the natural starting point for the stochastic simulation of a reaction network, e.g. using Gillespie's approach [52, 51, 48]. There, the exact time evolution of a spatially homogeneous mixture of molecular species, interacting through a specified set of coupled chemical reaction channels, is integrated numerically.

It is also possible to plug the Toy Model into existing reactors like Continuous-Stirred-Tank Reactors (CSTR) [92, 122], or Monte Carlo simulations [6]. As stochastic methods are particularly useful for stiff systems and systems with very small quantities, they are traditionally applied to biological systems. Chemical applications rather make use of the numerical integration of ordinary differential equations (ODE) to simulate the evolution of a CRN.

Using the rules of mass action kinetics [34, 64], the ODEs describing a network can be derived from the CRN while it is produced by the Toy Model [28]. The analysis of an ODE simulation can be further refined by methods such as chemical and statistical lumping, sensitivity analysis and systematic model reduction [43].

The Toy Model implements chemical reactions as explicit rewrite rules. In principle it is possible to simulate the collision of two molecules by assigning a collection of potential new bonds between them. Since the corresponding reactivity ΔE and the over-all reaction energy can be computed, one could in principle simulate reactions at this level. The computational cost would be immense, however. Nevertheless, one could use collision simulations to search for new reaction mechanism. This might be of particular interest when the Toy Model is used to explore "exotic chemistries" or chemical dynamics.

The energy calculation in the Toy Model includes a few empiric parameters (see appendix A). The parameters have been adjusted so as to reproduce the correct ordering of the chemical classes alkanes, alkenes and alkynes within an energy ranking of isomers. The parameters are bound to influence the enthalpy of reactions and may thus also affect the properties of the resulting CRN. The simulation of prebiotic chemistry can be executed with those parameters varying. The dependency of properties on these parameters could provide a measure for the stability and robustness of the network.

Other improvements and extensions of the three components (molecules, reactions, networks) of the Toy Model include for **molecules**:

(i) use the methods in [19] to accelerate the energy calculation, improve its accuracy by the methods of [4, 5, 94, 96],
(ii) implement cis/trans isomery using the SMILES "/\" notation,

for **reactions**:

(i) use the BEP/Hammond/Marcus equation for $\Delta E^{\ddagger}$ calculation, or derive it from the energy of intermediary transition structures,
(ii) parallelize the Toy Model by setting up one server per reaction ,
(iii) simulate catalysis by proteins, e.g. peptidase by catalytic triade, or by topological pharmacophore descriptors [74],
(iv) implement retrosynthetic steps [86, ch. 14.2] and common organic reactions (see appendix C) as rewrite rules,

for **networks**:

(i) use the planarity test [98] to limit networks (may not be sufficient),
(ii) submit simulated CRNs to classification [110],
(iii) simulate CRNs of organic catalysts [76] (e.g. polyenes), of other pre- or exobiotic chemistries [30] (e.g. tholin chemistry), of typical chemical engineering examples (e.g. polystyrene [125]), and of starburst molecules,

dendrimers and other polymers [80].

In summary, the Toy Model is now able to generate artificial chemistries and chemical reaction networks with few given parameters. The implementation is straightforward and intuitive, especially for the reaction simulation and the energy calculation. The latter is simple but more sophisticated than a biased knowledge-based calculation. The resulting networks can be used for exploring generic properties and their study may be extended to related areas.

Appendix A

Parameters

The energy calculation in the Toy Model is parametrized in terms of ionization energies I_j and overlap integrals S_{ij} of the usual Slater-type hybrid orbitals. The parameters S_{ij} needed for the energy calculation (see ch. 3) have been obtained from the tables in [81], using the formulae for the overlap of hybridized orbitals therein.

The bond lengths in tab. A.1, needed for this calculation were obtained from the atom radii in [57, vol. III, sect. 3.1.1] and further refined by comparison with [2].

Tab. A.2 lists the values of S_{ij} that apply to σ overlaps of hybridized orbitals that are oriented toward each other along a bond (upper left scheme in Fig. 3.4) and to π overlaps between p orbitals. The overlap integrals S_{ij} depend only on the type and orientation of the involved orbitals.

In the current implementation, the overlap parameters are arranged in a matrix `S` whose elements are lists of length 3. The rows and columns of the

Table A.1: Bond lengths depending on hybridization of bonding atoms. + indicates guessed values.

		H	C			N			O	
		s	sp^3	sp^2	sp	sp^3	sp^2	sp	sp^3	sp^2
H	s	0.74	1.01	1.07	1.056	1.01	1.02	+1.01	0.96	0.97
C	sp^3		1.54	1.52	1.46	1.47	+1.45	+1.43	1.43	+1.37
C	sp^2			1.34	1.32	+1.33	1.29	+1.26	+1.29	1.23
C	sp				1.21	+1.22	+1.19	1.15	+1.18	+1.12
N	sp^3					1.40	+1.32	1.25	1.30	+1.26
N	sp^2						1.24	+1.17	+1.22	1.18
N	sp							1.10	+1.15	+1.11

matrix obviously correspond to the type of the AO. The position in the list corresponds to the type of the overlap, where `S[0]` is a σ-overlap, `S[1]` is a π-, a hyperconjugation-, or an indirect overlap, and `S[2]` is a semi-direct or a fictitious overlap (see sect. 3.2).

Table A.2: Parameters for the graph orbital model. The top line gives the Coulomb integrals I for the atom orbitals that are currently implemented. Overlap integrals are listed separately for σ and π bonds. Semi-direct and indirect overlaps and banana-bonds in constrained rings are parametrized as the product of the bonding interaction with a scaling factor (see tab. 3.2).

σ		H	C			N			O	
		s	sp^3	sp^2	sp	sp^3	sp^2	sp	sp^3	sp^2
I		-13.6	-13.9	-14.5	-15.4	-16.6	-17.6	-19.7	-19.2	-20.6
H	s	0.75	0.69	0.65	0.66	0.62	0.63	0.63	0.55	0.57
C	sp^3	0.69	0.65	0.67	0.71	0.60	0.63	0.65	0.54	0.57
C	sp^2	0.65	0.67	0.77	0.80	0.70	0.73	0.77	0.64	0.68
C	sp	0.66	0.71	0.80	0.87	0.77	0.80	0.84	–	–
N	sp^3	0.62	0.60	0.70	0.77	0.58	0.61	0.65	0.63	0.67
N	sp^2	0.63	0.63	0.73	0.80	0.61	0.70	0.73	0.63	0.67
N	sp	0.63	0.65	0.77	0.84	0.65	0.73	0.82	–	–
O	sp^3	0.55	0.54	0.64	–	0.63	0.63	–	–	–
O	sp^2	0.57	0.57	0.68	–	0.67	0.67	–	–	–

π	C	N	O
	p	p	p
I	-11.4	-13.4	-14.8
C	0.38	0.31	0.26
N	0.31	0.31	0.26
O	0.26	0.26	0.26

Appendix B

GRW

GRW is implemented in `Haskell`, a lazy functional programming language [111]. Since it is not easy to glue together pieces of code written in functional and imperative programming languages (e.g. `C`), the engine is designed as client/server application. The client sends a graph to the server, which performs the rewrite step and sends the transformed graph back to the client. The rewrite behavior of the server only depends on the set of rewriting rules which are read from a file at server startup. This program architecture allows us to easily fit the rewrite engine to the needs of a particular task by simply changing the client. The server can be run in two rewriting modes: random rewrite and priority rewrite. In the former mode a rewrite rule is picked at random from the set of potentially applicable rules, while in the latter mode the rule with the highest "priority value" is chosen.

The graph rewrite rules are conveniently specified using the `Graph Meta Language` (GML) [90]. The specification of the Diels Alder reaction is, for example:

```
# Diels Alder
rule [
 context [
  node [ id 1 label "C" ]
  node [ id 2 label "C" ]
  node [ id 3 label "C" ]
  node [ id 4 label "C" ]
  node [ id 5 label "C" ]
  node [ id 6 label "C" ]
 ]
 left [
  edge [ source 1 target 2 label "=" ]
```

```
  edge [ source 2 target 3 label "-" ]
  edge [ source 3 target 4 label "=" ]
  edge [ source 5 target 6 label "=" ]
 ]
 right [
  edge [ source 1 target 2 label "-" ]
  edge [ source 2 target 3 label "=" ]
  edge [ source 3 target 4 label "-" ]
  edge [ source 4 target 5 label "-" ]
  edge [ source 5 target 6 label "-" ]
  edge [ source 6 target 1 label "-" ]
 ]
]
```

Appendix C

Organic reactions

From `http://www.liv.ac.uk/Chemistry/Links/reactions.html` and [86]:

- Ester Condensation
- Acryloin Condensation
- Aldol Condensation
- Baeyer-Villiger Rearrangement
- Beckmann Rearrangement
- Benzoin Condensation
- Birch Reduction
- Cannizzaro Reaction
- Chichibabin Reaction
- Claisen Condensation
- Claisen Rearrangement
- Cope Rearrangement
- Diels Alder Reaction
- Dienone Phenol Rearrangement
- Friedel Crafts Reaction
- Gabriel Synthesis
- Hell-Vollard-Zelimsky Halogenation
- Hofmann Rearrangement

- Kiliani-Fischer Synthesis
- Knoevenagel Condensation
- Koenigs-Knorr Synthesis
- Mannich Reaction
- Meerwein-Ponndorf-Verley Reduction
- Michael Condensation
- Reformatskii Reaction
- Wagner-Meerwein Rearrangement
- Wittig Reaction
- Wolff-Kishner Reduction
- Wurtz Reaction

or

- Basic/Nucleophilic
- Acidic/Electrophilic
- Electrophilic Aromatic Substitution (EAS),
- Radical
- Heterocyclic
- Pericyclic
- Oxidative/Reductive
- Carbene
- Organometallic
- Photochemical

Bibliography

[1] R. Albert and A.-L. Barabasi. Statistical mechanics of complex networks. *Rev. Mod. Phys.*, 74:47–97, 2002.

[2] N. W. Alcock. *Bonding and Structure.* Ellis Horwood, 1990. `http://www.iumsc.indiana.edu/radii.html`.

[3] L. A. N. Amaral, A. Scala, M. Barthelemy, and H. E. Stanley. Classes of small-world networks. *Proc. Nat. Acad. Sci.*, 97:11149–11152, 2000.

[4] A. B. Anderson. Electron density distribution functions and the ASED-MO theory. *Int. J. Quant. Chem.*, 49:581–589, 1994.

[5] A. B. Anderson and R. Hoffmann. Description of diatomic molecules using one lectron configuration energies with two-body interactions. *J. Chem. Phys.*, 60:4271–4273, 1974.

[6] A. P. Arkin. Synthetic cell biology. *Curr. Opin. Biotech.*, 12:638–644, 2001.

[7] L. Babai. *Lecture Notes in Computer Sciences : Fundamentals of Computation Theory*, chapter Moderately exponential bound for graph isomorphism, pages 34–50. Springer, 1981.

[8] R. J. Bagley and J. D. Farmer. Spontaneous emergence of a metabolism. In C. G. Langton, C. Taylor, J. D. Farmer, and S. Rasmussen, editors, *Artificial Life II*, pages 93–140, Redwood City, CA, 1992. Addison-Wesley.

[9] A. A. Balandin. *Multiplet theory of catalysis: Theory of hydrogenation. Classification of organic catalytic reactions. Algebra applied to strucutral chemistry*, volume 3. Moscow State Univ., 1970. in Russian.

[10] A.-L. Barabasi and R. Albert. Emergence of scaling in random networks. *Science*, 286:509–512, 1999.

[11] S. Benson. *Thermochemical kinetics: methods for the estimation of thermochemical data and rate parameters*. Wiley, New York, 1968.

[12] W. Braun, R. Fugmann, and W. Vaupel. Zur Dokumentation chemischer Forschungsgebiete. *Angew. Chem.*, 73:745–751, 1961.

[13] R. Breslow. On the mechanism of the Formose reaction. *Tetrahedron Lett.*, 21:22–26, 1959.

[14] A. C. Brown. On the theory of chemical combination. Master's thesis, University of Edinburgh, UK, 1864.

[15] A. Butlerow. Formation synthétique d'une substance sucrée. *C. R. Acad. Sci.*, 53:145–147, 1861.

[16] S. Cannizzaro. Über den der Benzoësäure entsprechenden Alkohol. *Liebigs Ann. Chem.*, 88:129–130, 1853.

[17] A. Cayley. On the mathematical theory of isomers. *Philos. Mag.*, 47:444–446, 1874.

[18] Computational chemistry comparison and benchmark database, release 6a, May 2002. `http://srdata.nist.gov/cccbdb/`.

[19] M. Challacombe. A simplified density matrix minimization for linear scaling self-consistent theory. *J. Chem. Phys.*, 110:2332–2342, 1999.

[20] A. Church. A set of pustulates for the foundation of logic. *Annals of Math. (2)*, 33:346–366, 1932.

[21] B. L. Clarke. Stoichiometric network analysis. *Cell Biophys.*, 12:237–253, 1988.

[22] D. C. Corneil and C. C. Gotlieb. An efficient algorithm for graph isomorphism. *J. ACM*, 17:51–64, 1970.

[23] C. J. Cramer and D. G. Truhlar. Implicit solvation models: Equilibria, structure, spectra, and dynamics. *Chem. Rev.*, 99:2161–2200, 1999.

[24] P. Decker, H. Schweer, and R. Pohlmann. Bioids. X. Identification of formose sugars, presumably prebiotic metabolites, using capillary gas chromatography/gas chromatography-mass spectroscopy of *n*-butoxime trifluoroacetates on OV-225J. *J. Chromatogr.*, 225:281–291, 1982.

[25] O. Diels and K. Alder. Synthesen in der hydroaromatischen Reihe. *Liebigs Ann. Chem.*, 460:98–122, 1928.

[26] P. Dittrich, J. Ziegler, and W. Banzhaf. Artificial chemistries - a review. *Artificial Life*, 7:225–275, 2001.

[27] P. Dittrich and W. Banzhaf. Self-evolution in a constructive binary string system. *Artificial Life*, 4:203–220, 1998.

[28] D. J. Dooling. Converting reaction mechanisms into ordinary differential equations suitable for integration. `http://winnie.chem-eng.nwu.edu/software/ode.html`.

[29] H. Dörr. *Efficient Graph Rewriting and Its Implementation*. Springer-Verlag, Berlin Heidelberg, 1995.

[30] K. Dose and H. Rauchfuss. *Chemische Evolution und der Ursprung lebender Systeme*. Wiss. Verlagges. Stuttgart, 1975.

[31] J. Dugundji and I. Ugi. An algebraic model of constitutional chemistry as a basis for chemical computer programs. *Top. Curr. Chem.*, 39:19–49, 1973.

[32] S. Ekins, M. J. de Groot, and J. P. Jones. Pharmacophore and three-dimensional quantitative structure activity relationship methods for modeling cytochrome P450 active sites. *Drug Metab. Disp.*, 29:936–944, 2001.

[33] J.-L. Faulon and A. G. Sault. Stochastic generator of chemical structure. 3. Reaction network generation. *J. Chem. Inf. Comput. Sci.*, 41:894–908, 2001.

[34] M. Feinberg. *Chemical Reactor Theory - A Review*, chapter Mathematical Aspects of Mass Action Kinetics. Prentice-Hall, Inglewood Cliffs, NJ, 1977.

[35] D. Fell. *Understanding the Control of Metabolism*. Number 2 in Frontiers in Metabolism. Portland Press, London, 1997.

[36] D. Fell and A. Wagner. The small world inside metabolic networks. *Proc. R. Soc. Lond. Ser. B*, 268:1803–1810, 2001.

[37] C. Flamm. Graph rewrite ?!@$+*. `http://www.tbi.univie.ac.at/Bled/Slides/xtof.pdf`, 2002.

[38] I. Fleming. *Frontier Orbitals and Organic Chemical Reactions*. Wiley: New York, 1976.

[39] E. Fontain and K. Reitsam. The generation of reaction networks with rain. Part 1. The reaction generator. *J. Chem. Inf. Comput. Sci.*, 31:96–100, 1991.

[40] W. Fontana. Algorithmic chemistry. In C. G. Langton, C. Taylor, J. D. Farmer, and S. Rasmussen, editors, *Proc. Workshop on Artificial Life (ALIFE '90)*, volume 5 of *Santa Fe Institute Studies in the Sciences of Complexity*, pages 159–210, Redwood City, CA, USA, Feb. 1992. Addison-Wesley.

[41] W. Fontana and L. W. Buss 'The arrival of the fittest': Toward a theory of biological organization. *Bull. Math. Biol.*, 56:1–64, 1994.

[42] W. Fontana and L. W. Buss The barrier of objects: From dynamical systems to bounded organization. In J. Casti and A. Karlqvist, editors, *Boundaries and Barriers*, pages 56–116, Redwood City, MA, 1996. Addison-Wesley.

[43] M. Frenklach. Modeling of large reaction systems. In J. Warnatz and W. Jäger, editors, *Complex chemical reaction systems, mathematical modelling and simulation*, volume 47 of *Springer Series in Chemical Physics*, pages 2–16. Springer-Verlag, Berlin, 1987.

[44] R. Fugmann. In *Proceedings of the IUPAC Congress 1959*, pages 331–341, 1959.

[45] S. Fujita. Description of organic reactions based on imaginary transition structures. 1. Introduction of new concepts. *J. Chem. Inf. Comput. Sci.*, 26:205–212, 1986.

[46] K. Fukui, T. Yonezawa, and H. Shingu. A molecular orbital theory of reactivity in aromatic hydrocarbons. *J. Chem. Phys.*, 20:722–725, 1952.

[47] N. W. Gabel and C. Ponnamperuma. Model for origin of monosaccharides. *Nature*, 216:452–455, 1967.

[48] C. W. Gardiner. *Handbook of Stochastic Methods*. Springer, Berlin, 1985.

[49] M. R. Garey and D. S. Johnson. *Computers and Intractability*. W. H. Freeman and Co., New York, 1979.

[50] J. Gasteiger and A. Herwig. Simulation of organic reactions: From the degradation of chemicals to combinatorial synthesis. *J. Chem. Inf. Comput. Sci.*, 40:482–494, 2000.

[51] M. A. Gibson and J. Bruck. Efficient exact stochastic simulation of chemical systems with many species and many channels. *J. Phys. Chem. A*, 104:1876–1889, 2000.

[52] D. T. Gillespie. Exact stochastic simulation of coupled chemical reactions. *J. Phys. Chem.*, 81:2340–2361, 1977.

[53] R. J. Gillespie and R. S. Nyholm. Inorganic stereochemistry. *Quart. Rev. Chem. Soc.*, 11:339–380, 1957.

[54] B. M. Gimarc and J. J. Ott. *Graph Theory and Topology in Chemistry*, chapter Graphs for chemical reaction networks: Applications to the isomerizations among the carboranes, pages 285–301. Elsevier, Amsterdam & New York, 1987.

[55] P. M. Gleiss, P. F. Stadler, A. Wagner, and D. A. Fell. Relevant cycles in chemical reaction networks. *Adv. Complex Syst.*, 4:207–226, 2001.

[56] I. Gutman, S. Klavžar, and B. Mohar, editors. *Fifty Years of the Wiener Index*, volume 35 of *MATCH*, 1997.

[57] E. Heilbronner and H. Bock. *Das HMO-Modell und seine Anwendung*. Verlag Chemie, Weinheim, 1970.

[58] R. Heinrich and S. Schuster. The modelling of metabolic systems. structure, control and optimality. *BioSystems*, 47:61–77, 1998.

[59] J. B. Hendrickson. Description of reactions: their logic and applications. *Recl. Trav. Chim. Pays-Bas*, 111:323–334, 1992.

[60] E. Hladká, J. Koča, M. Kratochvil, L. Matyska, J. Pospíchal, and V. Potůček. The synthon model and the program pegas for computer assisted organic synthesis. *Top. Curr. Chem.*, 166:121–197, 1993.

[61] I. L. Hofacker, W. Fontana, P. F. Stadler, L. S. Bonhoeffer, M. Tacker, and P. Schuster. Fast folding and comparison of RNA secondary structures. *Montash. Chem.*, 125:167–188, 1994.

[62] R. Hoffmann. An Extended Hückel Theory. I. Hydrocarbons. *J. Chem. Phys.*, 39:1397–1412, 1963.

[63] R. Hoffmann. An Extended Hückel Theory. III. compounds of boron and nitrogen. *J. Chem. Phys.*, 40:2474–2480, 1964.

[64] F. Horn and R. Jackson. General mass action kinetics. *Arch. Rat. Mech. Anal.*, 41:81–116, 1972.

[65] J. Howell, A. Rossi, D. Wallace, K. Haraki, and R. Hoffmann. ICON. *QCPE Bulletin*, 5, 1977.

[66] T. Ikegami and T. Hashimoto. Active mutation in self-reproducing networks of machines and tapes. *Artificial Life*, 2:305–318, 1995.

[67] F. Jensen. *Introduction to Computational Chemistry*. Wiley, Chichester, 1999.

[68] Y. Kanada. Combinatorial problem solving using randomized dynamic tunneling on a production system. In *1995 IEEE International Conference on Systems, Man and Cybernetics. Intelligent Systems for the 21st Century*, volume 4, pages 3784–9, New York, NY, 1995. IEEE.

[69] A. Kerber, R. Laue, and T. Wieland. Discrete mathematics for combinatorial chemistry. Workshop on Discrete Mathematics, Dimacs Center, NJ USA, 1998.

[70] R. B. King and D. H. Rouvray. A graph-theoretical interpretation of the bonding topology in polyhedral boranes, metal clusters and organic cations. *MATCH*, 7:273–287, 1979.

[71] G. Klopman. Chemical reactivity and the concept of charge- and frontier-controlled reactions. *J. Am. Chem. Soc.*, 90:223–243, 1968.

[72] J. Köbler, U. Schöning, and J. Torán. *The Graph Isomorphism Problem: Its Structural Complexity*. Birkhäuser, Basel, CH, 1993.

[73] J. Koča, M. Kratochvil, V. Kvasnička, L. Matyska, and J. Pospíchal. Synthon model of organic chemistry and synthesis design. *Lecture Notes in Chemistry*, 51, 1989.

[74] N. A. Kratochwil, W. Huber, F. Müller, M. Kansy, and P. R. Gerber. Predicting plasma protein binding of drugs : a new approach. *Bioch. Pharm.*, 64:1355–1374, 2002.

[75] D. Lancet, G. Glusman, D. Segré, O. Kedem, and Y. Pilpel Self-replication and chemical selection in primordial mutually catalytic sets. *Life and Evolution of the Biosphere*, 26:270–271, 1996.

[76] W. Langenbeck. Über organische Katalysatoren – L : Entwicklungslinien der organischen Katalysatoren. *Tetrahedron*, 3:185–196, 1958.

[77] E. Luks. Isomorphism of graphs of bounded valence can be tested in polynomial time. *J. Computer Syst. Sci*, 25:42–65, 1982.

[78] J. S. McCaskill and U. Niemann. Molecular graph reaction networks. In R. Hofestädt, T. Lengauer, M. Löffler, and D. Schomburg, editors, *Proc. of the German Conference on Bioinformatics*, pages 99–103, Leipzig, 1996. Univ. Leipzig.

[79] D. Mikulecky. Network thermodynamics and complexity: a transition to relational systems theory. *Comput. Chem.*, 25:369–391, 2001.

[80] F. Morgenroth and K. Müllen. Dendritic and hyperbranched polyphenylenes via a simple Diels-Alder route. *Tetrahedron*, 53:15349–15366, 1997.

[81] R. S. Mulliken, C. A. Rieke, D. Orloff, and H. Orloff. Formulas and numerical tables for overlap integrals. *J. Chem. Phys.*, 17:1248–1267, 1949.

[82] M. Nagl. *Graph-Grammatiken, Theorie, Implementierung, Anwendung*. Vieweg, Braunschweig, 1979.

[83] S. Patel, J. Rabone, S. Russell, J. Tissen, and W. Klaffke. Iterated reaction graphs: Simulating complex maillard reaction pathways. *J. Chem. Inf. Comput. Sci.*, 41:926–933, 2001.

[84] J. L. Pfaltz and A. Rosenfeld. Web grammars. In *Proc. Int. Joint Conference on Artificial Intelligence*, pages 609–619, 1969.

[85] E. Pfeil and H. Ruckert. Die Bildung von Zuckern aus Formaldehyd unter der Einwirkung von Laugen. *Liebigs Ann. Chem.*, 641:121–131, 1961.

[86] S. Pine, J. Hendrickson, D. Cram, and G. Hammmond. *Organische Chemie*. Vieweg, 1987.

[87] O. E. Polansky. Graphs in quantum chemistry. *MATCH*, 1:183–195, 1975.

[88] S. E. Prickett and M. L. Mavrovouniotis. Comstruction of complex reactions systems–I. Reaction description language. *Comp. Chem. Eng.*, 21:1219–1235, 1997.

[89] L. Radom. Structural consequences of hyperconjugation. *Prog. Theor. Org. Chem.*, 3:1–64, 1982.

[90] M. Raitner. GML file format. `http://www.infosun.fmi.uni-passau.de/Graphlet/GML/`.

[91] S. Rasmussen, C. Knudsen, R. Feldberg, and M. Hindsholm. The coreworld: Emergence and evolution of cooperative structures in a computational chemistry. *Physica D*, 42:111–134, 1990.

[92] J. B. Rawlings and J. G. Ekerdt. *Chemical Reactor Analysis and Design Fundamentals*. Nob Hill Publishing, 2002.

[93] R. C. Read. Every one a winner. *Annals of Discrete Math.*, 2:107–120, 1978.

[94] M. R. Repasky, J. Chandrasekhar, and W. L. Jorgensen. Improved semiempirical heats of formation through the use of bond and group equivalents. *J. Comp. Chem.*, 23:498–510, 2002.

[95] D. C. Roberts. A systematic approach to the classification and nomenclature of reaction mechanisms. *J. Org. Chem.*, 43:1473, 1978.

[96] E. Rousseau and D. Mathieu. Atom euqivalents for converting dft energies calculated on molecular mechanics structures to formation enthalpies. *J. Comp. Chem.*, 21:367–479, 2000.

[97] G. Rozenberg. *Handbook of Graph Grammars and Computing by Graph Transformation: Applications, Languages and Tools*. World Scientific Pub Co., 1999.

[98] C. Rücker and M. Meringer. How many organic compunds are gt-nonplanar? Talk held at MCC02.

[99] L. Salem. Intermolecular orbital theory of the interaction between conjugated systems. i. general theory ii. thermal and photochemical calculations. *J. Am. Chem. Soc.*, 90:543–552 and 553–566, 1968.

[100] C. Sandorfy. LCAO MO calculations on saturated hydrocarbons and their substituted derivatives. *Can. J. Chem.*, 33:1337, 1955.

[101] J. Sauer. Diels-Alder reactions Part II: The reaction mechanism. *Angew. Chem. Int. Ed.*, 6:16–33, 1967.

[102] S. Schuster, T. Dandekar, and D. A. Fell. Detection of elementary flux modes in biochemical networks: a promising tool for pathway analysis and metabolic engineering. *Tibtech*, 17:53–60, 1999.

[103] O. Sinanoğlu and K. B. Wiberg. *Sigma Molecular Orbital Theory*. Yale University Press, New Haven and London, 1970.

[104] J. C. Slater and G. F. Koster. Simplified LCAO Method for the periodic potential problem. *J. Chem. Phys.*, 94:1499–1524, 1954.

[105] G. P. Smith, D. M. Golden, M. Frenklach, N. W. Moriarty, B. Eiteneer, M. Goldenberg, C. T. Bowman, R. K. Hanson, S. Song, J. William C. Gardiner, V. V. Lissianski, and Z. Qin. Gri-mech 3.0. `http://www.me.berkeley.edu/gri_mech/`. GRI-Mech is essentially a list of elementary chemical reactions and associated rate constant expressions.

[106] G. N. Stephanopoulos, A. Aristidou, and J. Nielsen. *Metabolic Engineering: Principles and Methodologies*. Academic Press, San Diego, 1998.

[107] Y. Suzuki and H. Tanaka. Symbolic chemical system based on abstract rewriting and its behavior pattern. *Artificial Life and Robotics*, 1:211–219, 1997.

[108] J. J. Sylvester. On an application of the new atomic theory to the graphical representation of the invariants and covariants of binary quantics, with three appendices. *Amer. J. Math.*, 1:64–128, 1878.

[109] E. Szathmary. A classification of replicators and lambda-calculus models of biological organization. *Proc. R. Soc. Lond. Ser. B-Biol. Sci.*, 260:279–286, 1995.

[110] O. N. Temkin, A. V. Zeigarnik, and D. Bonchev. *Chemical Reaction Networks : a graph-theoretical approach*. CRC Press Boca Raton, FL USA, 1996.

[111] S. Thompson. ***Haskell****, The Craft of Functional Programming*. Addison-Wesley, Redwood City, CA, 2nd edition, 1999.

[112] A. M. Turing. Computability and λ-definability. *J. Symbolic Logic*, 2:153–163, 1937.

[113] I. Ugi, J. Bauer, K. Bley, A. Dengler, A. Dietz, E. Fontain, B. Gruber, R. Herges, M. K. abd Klaus Reitsam, and N. Stein. Computer unterstützte direkte Lösung chemischer Probleme - die Entstehungsgeschichte und gegenwärtiger Status einer neuen Disziplin der Chemie. *Angew. Chem.*, 105:210–239, 1993.

[114] I. Ugi, N. Stein, M. Knauer, B. Gruber, and K. Bley. New elements in the representation of the logical structure of chemistry by qualitative mathematicals models of corresponding data structures. *Top. Curr. Chem.*, 166:199–233, 1993.

[115] H. Urey and S. L. Miller. Organic compound synthesis on the primitive earth. *Science*, 130:245–251, 1959.

[116] J. Vollmer. Wiswesser Line-formula chemical Notation (WLN): an introduction. *J. Chem. Educ.*, 80:192–196, 1983.

[117] S. Wasserman and K. Faust. *Social Network Analysis*. Cambridge University Press, 1994.

[118] D. J. Watts. *Small Worlds*. Princeton University Press, Princeton NJ, 1999.

[119] D. J. Watts and S. H. Strogatz. Collective dynamics of 'small-world' networks. *Nature*, 393:440–442, 1998.

[120] D. Weininger. SMILES, a chemical language and information system. *J. Chem. Inf. Comput. Sci.*, 28:31–36, 1988.

[121] D. Weininger, A. Weininger, and J. Weininger. SMILES. 2. Algorithm for generation of unique SMILES notation. *J. Chem. Inf. Comput. Sci.*, 29:97–101, 1989.

[122] A. Wernitznig. *RNA Optimization in Flow Reactors: A study in silico*. PhD thesis, University of Vienna, 2001.

[123] H. Wiener. Structure determination of paraffine boiling points. *J. Am. Chem. Soc.*, 69:17–20, 1947.

[124] J. H. Wilkinson. *The Algebraic Eigenvalue Problem*. Clarendon Press, Oxford, 1965.

[125] M. J. D. Witt, D. J. Dooling, , and L. J. Broadbelt. Computer generation of reaction mechanisms using quantitative rate information: Application to long-chain hydrocarbon pyrolysis. *Ind. Eng. Chem. Res.*, 39:2228–2237, 2000.

[126] R. Woodward and R. Hoffmann. The conservation of orbital symmetry. *Angew. Chem. Int. Ed. Engl.*, 8:781–853, 1969.

[127] M. A. Wurtz. Sur un aldéhyde-alcool. *Bull. Soc. Chim. Fr.*, 17:426–442, 1872.

[128] T. Yamamoto and K. Kaneko. Tile automaton: A model for an architecture of a living system. *Artif. Life*, 5:37–76, 1999.

[129] J. Yang. Goforth. `http://www.daylight.com/meetings/emug99/Yang/goforth/index.html`, 1999.

[130] S. Yoshii, H. Inayoshi, and Y. Kakazu. Atomoid: A new prospect in reaction-formation system spontanous hypercycle guided by dissipative structural properties. In C. Langton and K. Shimohara, editors, *Artificial Life V*, pages 418–425, Cambridge, MA, 1997. MIT Press.

[131] A. V. Zeigarnik. On hypercycles and hypercircuits in hypergraphs. In P. Hansen, P. W. Fowler, and M. Zheng, editors, *Discrete Mathematical Chemistry*, volume 51 of *DIMACS series in discrete mathematics and theoretical computer science*, pages 377–383, Providence, RI, 2000. American Mathematical Society.

[132] A. V. Zeigarnik and O. N. Temkin. A graph-theoretic model of complex reaction mechanisms: bipartite graphs and the stoichiometry of complex reactions. *Kinet. Catal. Engl. Transl.*, 35:691–701, 1994.

Curriculum vitae

Personal details

Name: Gil BENKÖ

Date of Birth: 16 August 1979

Nationality: Austrian

Education

1998 – 2002 Diploma studies in chemistry
Thesis: A toy model of chemical reaction networks
University of Vienna, Austria

1997 – 1998 Undergraduate mathematics, physics, chemistry and CS
EURINSA Scientific and Technical University, Lyon, France

1997 Austrian Matura and French Scientific Baccalauréat
(with distinction)
Lycée Français, Vienna, Austria

Practical experience

04 – 07/2001 Sequence analysis of human G-protein coupled receptors
Roche Bioscience, Palo Alto, CA USA

07 – 09/2000 pKa prediction with the Daylight Toolkit/Oracle database
F. Hoffmann–La Roche, Basel, Switzerland

07 – 08/1999 Molecular biology lab
Hoechst Marion Roussel, Frankfurt, Germany

09/1998 Creation of a database/molecular biology lab
IAEA Agriculture and Biotechnology, Seibersdorf, Austria

Presentations

Talk: A toy model of chemical reaction networks
MATH/CHEM/COMP 2002

Poster: Reactions of 5-substituted adamantylidenes in zeolite Y
Austrian Chemistry Days 2002

The Wooing of Archibald

Modern trends like latex coatings on maize basis quickly contrive to recruit adepts among the honoured members of the Drones Club. Thus only a dead-head would have tried to investigate the flexible-dress-code's reason. Clad in clothes of some foreign latex-like material, the gentlemen seemed to test with all their energy the performance of their transpiration. A Gin-and-Ginger-Ale, positive about reversing osmosis, found a twin soul in the prune.
Just as another endothelium was about to join the epithelium's swelling state, Mr Mulliner shook his head.
'I cannot agree with you, gentlemen. If those coatings had any real future, insects would have exchanged their chitin carapace for them since long ago. My authority on this subject stems from my efforts to promote the nuptial aggregation of my nephew Archibald and Aurelia Cammarleigh, for which the bridegroom rewarded me with biochemical literature.'
'Golly!' ventured to comment a Whisky-and-Water, slightly inebriated by the essence of the joined efforts of incubated barley and rye.

My nephew Archibald [said Mr Mulliner] established his reputation as a brilliant biochemist during his works on the repetitive regions in the TRαY-group root factor, a plasma protein, or something like this.
As he saw Aurelia Cammarleigh first through his tortoiseshell-rimmed glasses, love went on all over him like rooting hormone. The effect was comparable to a brain graft from a hen, so he was not aware of my helpful presence. After his blood had nearly coagulated, he gave his fibrinogen a rest and gasped:
'Never seen such a divine egg in the whole literature!'
Seeing that he was not alone, he regained control over himself and refocused his concentration on me.
'Is my specificity for this superb ligand reciprocated? The cry goes round Kensington 'The pathway to Aurelia's heart is as blocked as if stuffed with polyacrylamide and PVC!',' he told me.
'Apparently, being hit by Amor's pollen sends your cerebral nodules centrifuging,' I said. 'Don't let that love-at-first-sight tag on your forehead

affect the general wisdom that lies in our genes. I have already activated the necessary neuronal structures, that I fertilize, by the way, every morning by soja shoots and cereals, notably Real Buck U'Uppo Power Oats&Wheat.'
I pointed out to him that chicks like Aurelia would be the most impressed on by divine disposition, even more than by intravenous auxin. Furthermore, we knew that the number of petals of a blossom was even for dicotyledons and odd for monocotyledons. Adding 1+1, the rest was simple, provided that he supplied her with enough monocotyledons. After consulting the ripping-petals-off-a-blossom oracle ('I love him, I don't, I love him, I don't,...'), she would have to fulfil her destiny.
I could see his face's expression relax as the blood sodium choride concentration resumed the physiological level in his veins.

As he quickly walked away to her, I hoped that, for the sake of a stable and viable marriage, he wouldn't let his strong love be eluted by her daily increasing logorrhea, and cherish its filtrate.